

## Orthographic analysis of geological structures—I. Deformation theory

DECLAN G. DE PAOR\*

Department of Geology, University College, Galway, Ireland

(Received 1 July 1982; accepted in revised form 11 March 1983)

**Abstract**—Orthographic projection transforms a three-dimensional object into its two-dimensional image by a mechanism of homogeneous deformation, with infinite shortening along the parallel projection lines. The orthographic orientation net is therefore a useful tool for the analysis of rank-2 tensor operations such as deformation and displacement. A tensor transforms orthogonal radii of the unit sphere into conjugate radii of an ellipsoid, here termed the tensor's ellipsoid. In two dimensions, any symmetric or asymmetric tensor's ellipse may be represented by a great circle on the orthographic orientation net or by a Mohr circle, generally in an 'off-axis' position. The Mohr circle's points of intersection with its reference axis define the tensor's eigenvectors and eigenvalues, which may be real or complex. An asymmetric tensor's eigenvectors are not mutually orthogonal, nor do they parallel the principal semi-axes of the tensor's ellipse. These facts are used to classify plane deformations. Any rotational deformation may be factored using Mohr circles for polar or additive decomposition.

In three dimensions, a symmetric or asymmetric tensor's ellipsoid may be represented by a graticule on the orthonet with the aid of polar decomposition. The two-dimensional tensor and ellipse corresponding to any section of the three-dimensional state may be determined from a skiodrome.

In order to apply rank-2 tensor concepts to heterogeneous deformation, a way of describing the gradients of rank-2 tensors (i.e. their variation with position in the heterogeneous tensor field) is needed. A rank-3 tensor serves this purpose.

### INTRODUCTION

#### *Orthographic projection*

TWO TYPES of orientation net are commonly used in the analysis of geological data. They are the stereonet which conserves angle, and the equal-area Schmidt net (Phillips 1954). The orthographic net, or orthonet, has been available to geologists since the work of Wright (1911) but its uses appear to have been confined to drawing crystals (Hilton 1917), skiodromes (projections of curves of equal velocity in optical minerals, Wahlstrom 1951) and block diagrams (McIntyre & Weiss 1956, Ragan 1973, Lisle 1982).

A block diagram is interpreted by the human eye as an oblique view of a solid body in space, commonly a map and two orthogonal sections. Actually, the block diagram is confined to the plane of the figure and its 'sides' can be obtained by application of finite homogeneous deformations to the map and sections. The effects of deformation and tilting are indistinguishable when the tilted plane is viewed orthographically. This equivalence permits the orthonet to be used in a variety of structural applications, not only as a graphical aid to visualization but also as a means of discovering algebraic solutions to problems (e.g. De Paor 1981a, b). It may prove as powerful an analytic tool in the future as the stereonet did in the past.

An orthonet is obtained by projecting a sphere onto the plane in such a way that all lines of projection are perpendicular to the plane. Its great and small circles are

actually ellipses, though the small circles are viewed 'edge-on' in the equatorial projection of Fig. 1 and therefore appear as straight line segments. In full spherical projection, a plane of dip  $\delta$  and strike  $\sigma$  is represented by an ellipse of axial ratio  $\sec \delta$  and long axis orientation  $\sigma$  (the lower and upper hemisphere parts may be distinguished by ornament). A line of plunge  $\phi$  and trend  $\theta$  is represented by a point with polar coordinates  $(P \cos \phi, \theta)$  equivalent to Cartesian coordinates  $(Pl, Pm)$  where  $l, m$  are direction cosines of the line and  $P$  is the radius of the net. Furthermore, a vector of magnitude  $V$  in the direction of the above line may be represented by an arrow which 'pierces' the sphere at  $P \cos \phi$  from the centre of the projection and continues in the  $\theta$ -direction to a distance  $V \cos \phi$  from the centre (Fig. 2) (De Paor 1979).

#### *Deformation nomenclature*

Truesdell & Toupin (1960 p. 243) defined deformation as the transformation of a portion of matter from one configuration to another. On p. 255, citing Rankine (1851) they described strain loosely as the change in length and relative direction occasioned by deformation. Deformation and strain are synonymous in much of the geological literature (e.g. Flinn 1962, Ramsay 1967). In this paper the coordinate origin shifts with a material point and the reference frame is therefore insensitive to homogeneous translation. Deformation here refers to any combination of stretch and rotation whereas strain refers to any *change* in relative length (longitudinal strain) or relative direction (shear strain). The term strain ellipse is a misnomer because the ellipse in question does not describe a change in configuration but rather a final configuration.

\* Present address: The Department of Earth and Planetary Sciences, The Johns Hopkins University, Baltimore, MD 21218, U.S.A.

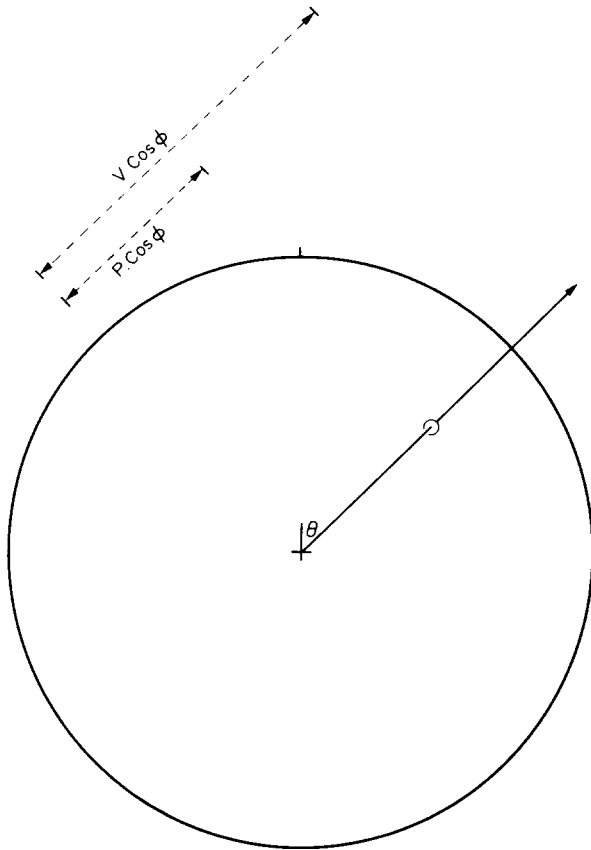


Fig. 2. Projection of a vector on the orientation net. ( $V, \theta, \phi$ ) are the vector's polar coordinates.  $P$  is the net's radius.

In a domain of homogeneous rotational deformation let a unit vector  $I$  join two material points. The deformed equivalent of  $I$  is here defined as the deformation vector  $D$ . Relative to  $I$ , its polar coordinates are  $(S, \alpha)$ , the stretch and rotation of  $I$ . For the special case of irrotational deformation, the deformed equivalent of  $I$  is here defined as the stretch vector  $S$ . Its polar coordinates are  $(S, \rho)$ , the stretch and passive rotation of  $I$ . The maximum, minimax and minimum values of  $S$  are labeled  $X, Y$  and  $Z$ , respectively (Ramsay 1967, p. 130).

$D$ , or in the special case  $S$ , may be resolved into a normal component  $N$  parallel to  $I$  and a coplanar transverse component  $T$  perpendicular to  $I$  (Ericksen 1960 p. 844 uses normal and shear components analogously).

Natural strain  $\epsilon$  and extension  $e$  are conventionally defined as

$$\begin{aligned} \epsilon &= \ln(S) \\ e &= S - 1. \end{aligned} \tag{1}$$

Elongation  $\epsilon$  is here defined as

$$\epsilon = N - 1 \tag{2}$$

in accord with Truesdell & Toupin (1960 p. 256) but not Ramsay (1967 p. 52). The quadratic stretch  $\lambda$  is defined as

$$\lambda = S^2. \tag{3}$$

The displacement vector  $U$  is here defined as the change in an initial unit vector  $I$ ,

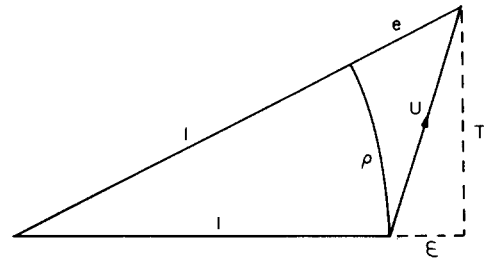


Fig. 3. Stretch and displacement notation for a line of initial length  $l$  and stretched length  $l + e$ .  $U$  is the displacement vector; its normal and transverse components are  $\epsilon$  and  $T$ .  $P$  is the line's rotation in radians.

$$U = D - I \tag{4}$$

in general, or

$$U = S - I, \tag{5}$$

if the deformation is irrotational (Malvern 1969 used the term unit relative displacement). The components of  $U$  are  $(\epsilon, T)$  (Fig. 3).

The maximum, minimax and minimum values of any of the scalar parameters above are hereby termed principal values. The corresponding vectors are termed principal vectors.

Relative to the direction of an arbitrary deformation vector  $D$ , the material in any perpendicular plane before deformation will be sheared through an angle  $\psi$  whose tangent  $\gamma$  is here defined as the geological shear strain of  $I$ . (Truesdell & Toupin 1960, p. 256, used the symbol  $\gamma$  and term shear to denote the decrease in angle between any two lines, not necessarily initially orthogonal.) Where there is no fear of confusion with infinitesimal engineering shear strain (e.g. Malvern 1969, p. 121) or finite classical shear strain (e.g. Truesdell & Toupin p. 267), the prefix 'geological' may be discarded.

In response to a simple torsion, material may become heterogeneously twisted about a discrete straight line. In the absence of any other superposed deformation, the angular twist  $\chi$  of a discrete unit vector  $I$  is here defined as the angular deflection of any vector initially parallel to  $I$  and the twist strain  $\Gamma$  is defined as

$$\Gamma = \tan \chi \tag{6}$$

(compare Truesdell & Toupin 1960, p. 298).

Homogeneous deformation and displacement are types of (rank-2) tensor. I propose to define a Cartesian tensor as an operator which transforms orthogonal radii of the unit sphere into conjugate radii of an ellipsoid (three ellipsoid radii are conjugate if the tangent plane at any one parallels the other two).

Simple examples of tensors, written as rows of column vectors, include the identity tensor

$$\begin{aligned} \mathbf{I} &= [I_1 \ I_2 \ I_3] \\ &= \begin{bmatrix} 1 & 0 & 0 \\ 0 & 1 & 0 \\ 0 & 0 & 1 \end{bmatrix} \end{aligned} \tag{7}$$

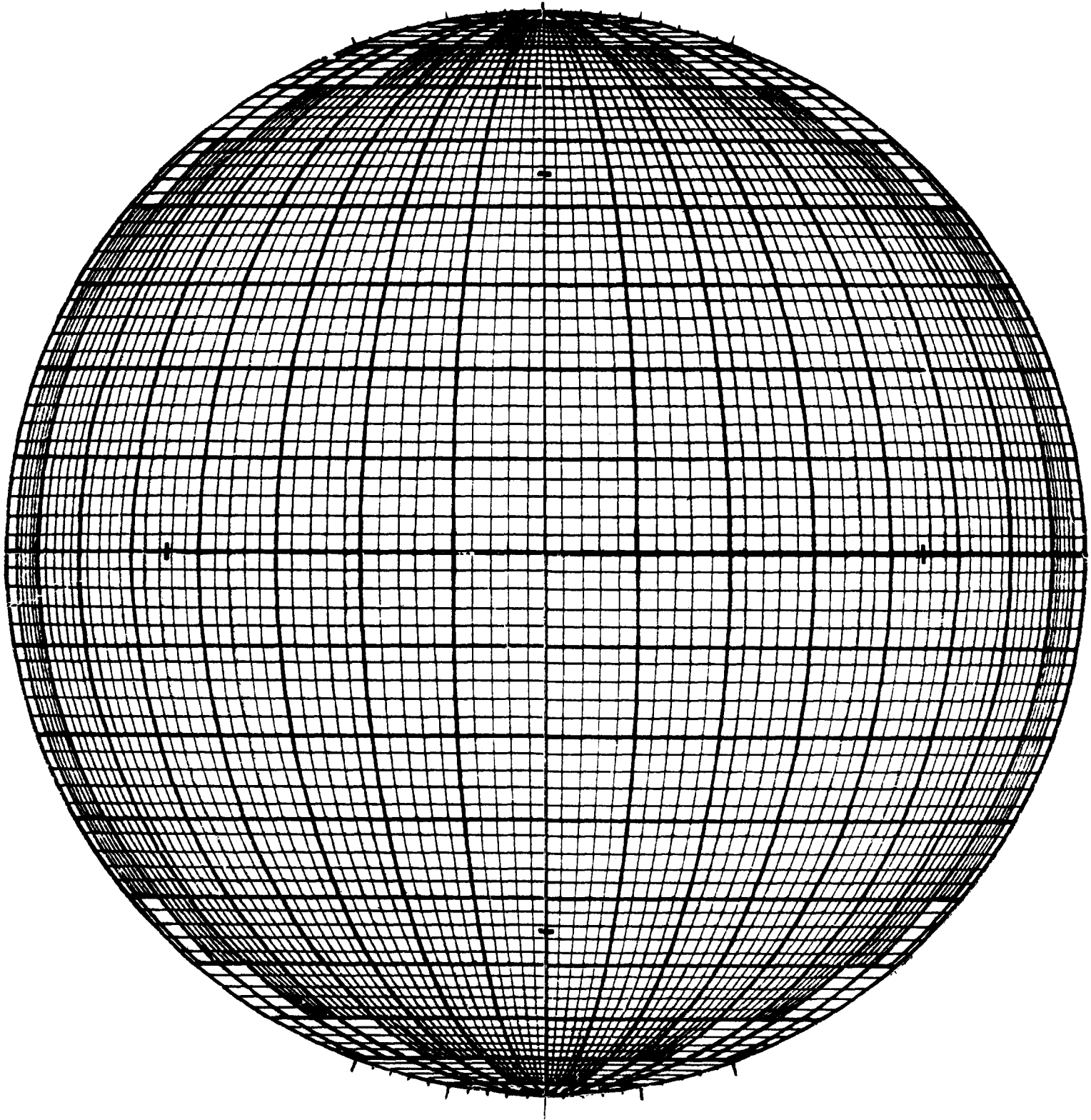


Fig. 1. An equatorial orthographic net. The radius is 10 cm.



which identifies the base vectors  $I_j (j = 1, 2, 3)$ , the tensor

$$\mathbf{M} = M\mathbf{I}, \tag{8}$$

where  $M$  is a scalar magnification factor and the rotation tensor

$$\begin{aligned} \mathbf{R} &= [\mathbf{R}_1 \quad \mathbf{R}_2 \quad \mathbf{R}_3] \\ &= \begin{bmatrix} l_1 & l_2 & l_3 \\ m_1 & m_2 & m_3 \\ n_1 & n_2 & n_3 \end{bmatrix}, \end{aligned} \tag{9}$$

where  $\mathbf{R}_j$  are an orthonormal triad with direction cosines  $l_j, m_j, n_j$ .

In general,  $\mathbf{V}$  is a tensor if, for all  $\mathbf{R}$ ,  $\mathbf{VR}$  are conjugate radii of an ellipsoid, here termed the tensor's ellipsoid. The tensor's ellipsoid is fixed in space, so that, if the reference frame is changed from  $\mathbf{I}$  to  $\mathbf{R}$  the conjugate radii  $\mathbf{VR}$  appear to be rotated through  $\mathbf{R}^{-1}$  to become  $\mathbf{R}^{-1}\mathbf{VR}$ . These are the transformed base vectors,  $\mathbf{V}'$  of the new (primed) reference frame, so that

$$\mathbf{V}' = \mathbf{R}^{-1}\mathbf{VR}. \tag{10}$$

Thus, the unconventional definition of a tensor proposed here leads to the conventional tensor transformation rule, equation (10).

The intimate relationship between a tensor and its ellipsoid is fundamental to the method of orthographic analysis. This relationship does not appear to have been described before, although Nye (1951 p. 47) and Flinn (1979) discussed the special case of a positive definite symmetric tensor's representation quadric, and Truesdell & Toupin (1960, pp. 250–253 and p. 552) reviewed more complicated quadrics which have been used to represent symmetric tensors geometrically since the unpublished work of Fresnel in 1822.

If  $\mathbf{V}$  is non-singular (that is, if its column vectors are not coplanar) it has an inverse  $\mathbf{V}^{-1}$  which transforms orthogonal radii of the unit sphere into conjugate radii of  $\mathbf{V}$ 's reciprocal ellipsoid. Therefore,  $\mathbf{V}$  transforms conjugate radii of its reciprocal ellipsoid into orthogonal radii of the unit sphere. We now define a tensor's left and right principal directions as the axial directions of its ellipsoid and reciprocal ellipsoid, respectively (this is consistent with Truesdell & Toupin 1960, p. 261). It should be clear that a tensor must transform its right principal directions into its left principal directions, there being only one set of lines which are orthogonal before and after transformation.

Every tensor  $\mathbf{V}$  transforms at least one unit vector  $\mathbf{R}$  without rotation so that  $\mathbf{VR}$  and  $\mathbf{R}$  are parallel (Thompson & Tait 1867).  $\mathbf{R}$  is then called an eigenvector and the magnitude of  $\mathbf{VR}$  is the corresponding eigenvalue.

In this paper, tensors are named and labelled consistently according to the physical significance of their ellipsoid's principal semi-axes. This rule sometimes permits a choice of logical names (for example, stress tensor or normal stress tensor) but unnecessary new terminology is avoided.

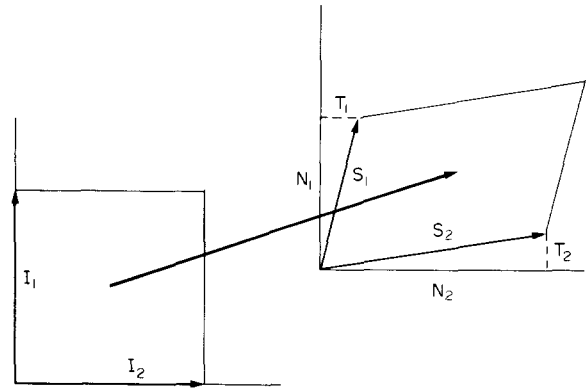


Fig. 4. The stretch tensor  $[S_1 \ S_2]$  transforms the arbitrary unit square  $[I_1 \ I_2]$  into a parallelogram. The reference frame is insensitive to the translation (bold arrow). Note the equality of the off-diagonal components  $T_1$  and  $T_2$ .

### THE STRETCH TENSOR AND ELLIPSOID

#### Two-dimensional analysis

For a homogeneous irrotational deformation in two dimensions, it follows from the above that the stretch ellipse may be defined simply as the deformed shape of an initial unit circle and similarly that the stretch tensor may be defined as the symmetric tensor whose column vectors define the deformed sides of an initial unit square. Using the reference axes  $I_j$  as adjacent sides of the initial unit square, the corresponding sides of the deformed square may be specified by their stretch vectors  $S_j$ . These form the columns of the stretch tensor,

$$\mathbf{S} = [S_1 \ S_2] \tag{11}$$

as illustrated in Fig. 4. Each column vector may be expanded in terms of its normal and transverse components,

$$\mathbf{S} = \begin{bmatrix} N_1 & T \\ T & N_2 \end{bmatrix}, \tag{12}$$

the transverse components being equal because of the irrotational nature of the deformation. Of course the shape of a deformed square, and thus the components of its stretch tensor, depends on the choice of  $I_j$ .

Tensors have a major advantage over ellipses: the parallelograms they describe may be used to 'tile' the plane, permitting rapid correlation of pre- and post-deformation coordinates.

Choi & Hsü (1971), De Paor (1981a, b) and Means (1982) have described a Mohr circle for stretch. The Mohr circle (Fig. 5) is centred at  $\frac{1}{2}(N_1 + N_2)$  and passes through the points  $(N_1, T)$  and  $(N_2, -T)$ . The attitude  $\theta$  of the semi-major stretch  $X$  is given by

$$\tan 2\theta = \frac{2T}{N_1 - N_2} \tag{13}$$

while the principal stretches  $X, Y$  are respectively

$$\frac{1}{2}(N_1 + N_2) \pm \frac{1}{2}(N_1 - N_2) \sec 2\theta. \tag{14}$$

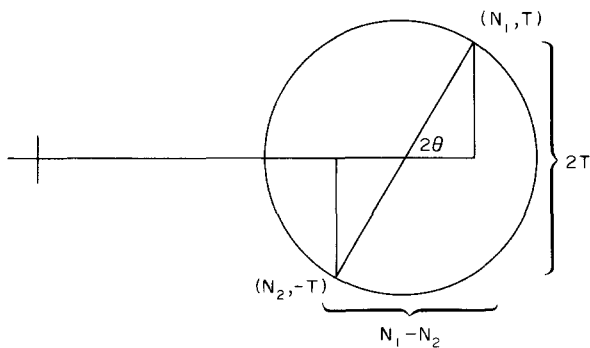


Fig. 5. A Mohr construction for stretch. See text for details.

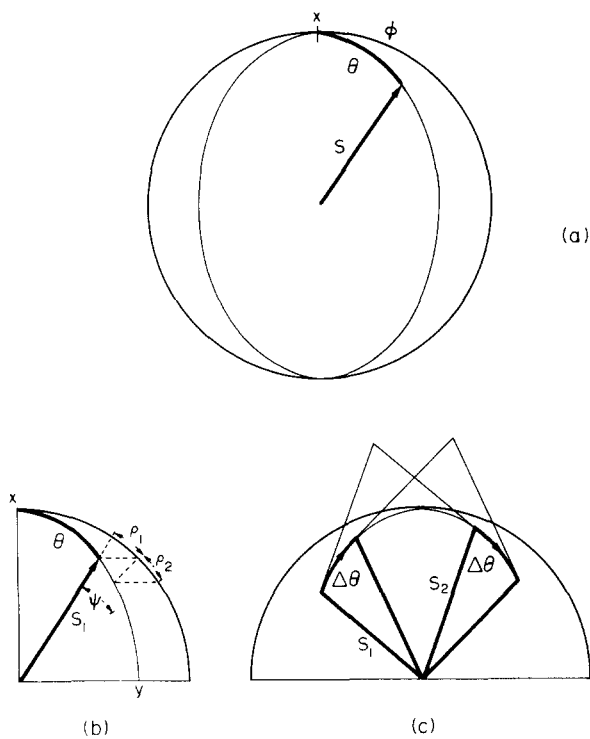


Fig. 6. (a) Orthographic construction for stretch. *S* is the radius vector at  $\phi$  to the *X*-direction. It was initially at  $\theta$  to *X*. (b) Definition of angular shear  $\psi$  in terms of the passive rotations  $\rho_1$  and  $\rho_2$ . See text. (c) Graphic solution of the tensor transformation rule, for a rotation of the reference frame through  $\Delta\theta$ .

A much simpler representation of stretch is achieved with the aid of the orthonet (Fig. 6). An elliptical great circle to represent the deformed state is chosen by rotating the net axis through  $\theta$  and tilting the primitive circle through the arcsecant of  $X/Y$ . Since the radius of the net now represents the principal stretch  $X$ , a circle of radius  $\sqrt{XY}$  may be drawn to represent the initial state. The stretch in the direction at  $\phi$  to the *X*-direction after deformation is obtained by setting off a true angle  $\phi$  from *X* and reading the corresponding radius of the great circle, this being equivalent to solving the polar equation of an ellipse,

$$\lambda^{-1} = \lambda_X^{-1} \cos^2 \phi + \lambda_Y^{-1} \sin^2 \phi. \quad (15)$$

The stretch vector corresponding to the direction initially at  $\theta$  to *X* is obtained by setting off  $\theta$  as if it were a

pitch on the great circle (Fig. 6), this being equivalent to solving

$$\lambda = \lambda_X \cos^2 \theta + \lambda_Y \sin^2 \theta \quad (16)$$

(Ramsay 1967, p. 65). The angle  $\rho_1$ , through which the  $\theta$ -direction is passively rotated while stretching, and angle  $\rho_2$ , through which some direction rotates to become the  $\theta$ -direction, can be read off the construction. Their sum gives the angular shear  $\psi$  of the  $\theta$ -direction because, for irrotational deformation, the reciprocal rotation of any direction is numerically equal to the forward rotation of a perpendicular direction (Ramberg 1975).

The stretch tensor *S* is represented in Fig. 6. Its Cartesian components are obtained by projection onto the directions of  $I_1$  and  $I_2$  which make true angles of  $\theta$  and  $\theta - \pi$  with *X*. The tensor's reference frame is rotated through an angle  $\Delta\theta$  by rotating the column vectors  $S_j$  through a pitch angle of  $\Delta\theta$  on the chosen great circle, which is equivalent to solving equation (5). If the rotation were applied to the vectors  $S_j$  but not their reference axes  $I_j$ , the deformation described would be rotational (see below).

The relationship between the orthographic and Mohr-circle constructions is illustrated in Fig. 7, as presented to the Tectonic Studies Group A.G.M., Nottingham, 1979. The basic geometric features appear in the work of De la Hire (1685, see Fig. 7b) although the latter author was clearly unaware of the mechanical implications. Figure 7 enables one to derive, directly, the equations of the Mohr circle for stretch (Choi & Hsü 1971, De Paor 1981a, b, Means 1982), identify the correct sign conventions and locate the Mohr circle's pole (e.g. Malvern 1969, p. 110). Figure 8 justifies the use of 'off-axis' Mohr circles for the analysis of rotational deformations (De Paor 1981a, b, Means this issue).

In the case of pure shear, the principal stretches are reciprocal and therefore the principal natural strains may be written

$$\epsilon = \ln(X) \quad (17)$$

$$-\epsilon = \ln(1/X). \quad (18)$$

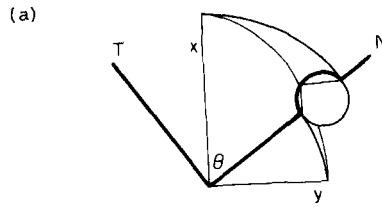
Thus the Mohr circle for stretch is centred at  $\cosh(\epsilon)$  and has a radius of  $\sinh(\epsilon)$ . The stretch tensor may therefore be written in the format

$$\mathbf{S} = \begin{bmatrix} \cosh(\epsilon) + \sinh(\epsilon) \cos 2\theta & \sinh(\epsilon) \sin 2\theta \\ \sinh(\epsilon) \sin 2\theta & \cosh(\epsilon) - \sinh(\epsilon) \cos 2\theta \end{bmatrix} \quad (19)$$

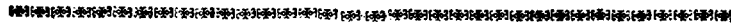
for a reference frame at  $\theta$  to the principal directions (Fig. 9). The product moment of *S* is seen to be equivalent to Elliott's (1970) shape factor. The importance of this format is that the tensor is described entirely in terms of its own principal vectors, without reference to parameters of the reference axes, which are unknown but probably very complex functions of the natural strains of those axes.

### Three-dimensional analysis

The three-dimensional Mohr construction (e.g. Ramsay 1967, p. 150) is cumbersome and so is rarely used.



(b)



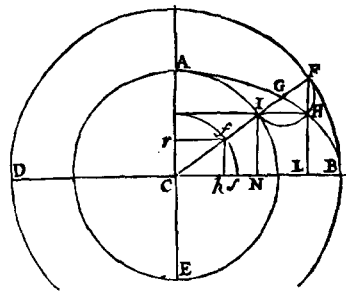
PROPOSITIO IV.

PROBLEMA.

Quolibet puncta lineæ Ellipticæ reperire, cujus dati sunt axes AE, BD, & centrum C.

Centro C & semidiametro CD describatur circulus BFD; similiter centro C & semidiametro CA circulus AIE; per centrum commune C ductâ diametro qualibet CIF occurrente circulis in I & F, super rectâ IF pro diametro fiat circulus FHI, cujus centrum G, ducaturque FL rectâ perpendicularis à puncto F ad DB, & occurrens circulo FHI in H; dico punctum H esse ad Ellipsim quaesitam.

Junctis I H punctis, angulus IHF erit rectus propter semicirculum, ideoque IH erit parallela CB; & propter similia triangula, ut quadratum CF, vel CB ad quadratum CI, vel CA, sic quadratum FL, quod æquale est rectangulo DL, IB propter circulum DFB, ad quadratum IN vel HL; quamobrem punctum H erit ad Ellipsim, cujus dati sunt axes per tertiam propositionem tertii libri, & cum sit eadem demonstratio



pro quibuscunque aliis punctis, factum est propositum.

COROLLARIUM.

Patet idem exequi posse sine circulo FHI; nam à puncto F ductâ perpendiculari FL ad CB, & à puncto I rectâ IH parallelâ CB, & occurren-

te FL in H, erit punctum H ad Ellipsim, ut supra ostendimus.



Fig. 7. (a) Relationship between Mohr and orthographic constructions for stretch. Arcs of circles are of radius  $X$  and  $Y$ . The inscribed right-angle defines the principal directions. (b) Extract from De la Hire (*Sectiones Conicæ in Novem Libros Distributæ*, 1685).  $FHI$  is the Mohr semicircle for the ellipse  $AHB$ .  $H$  is opposite the pole of the Mohr circle.

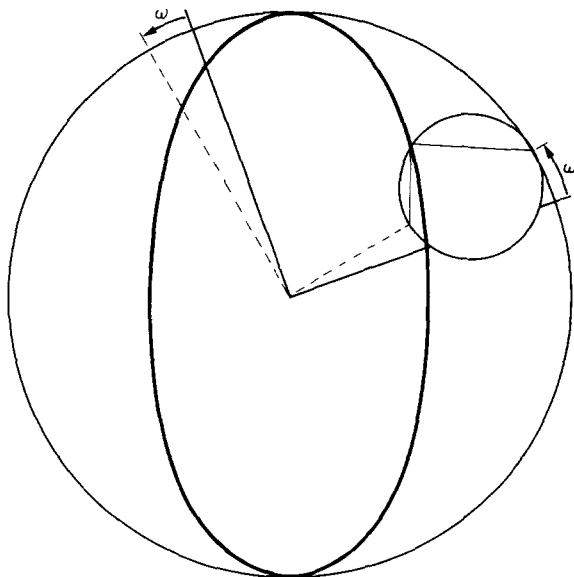


Fig. 8. Orthographic and Mohr constructions for rotational deformations.  $\omega$ , which is negative in this case, is the rotation experienced prior to stretch (dashed axes). The Mohr circle is 'off-axis' (Means this issue) relative to the bold reference frame.

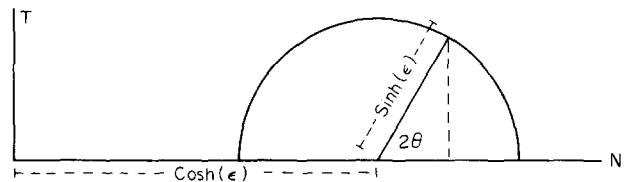


Fig. 9. Mohr circle for constant area stretch expressed in terms of the principal natural strain  $\epsilon$ .

The analogous orthographic construction for stretch in three dimensions is developed by considering first the theoretical case where the stretch along  $X$  is unity and the shortening along  $Z$  is infinite, so that the stretch ellipsoid becomes squashed into the  $XY$ -plane and occupies the area bounded by the ellipse of axial ratio  $X/Y$  (Fig. 10). Now the stretch of the arbitrary unit vector  $I$  (a radius of the net in this case) is obtained by moving the tip of  $I$  along its latitude line till it is brought closer to the  $X$ -axis by a factor  $Y$ .

To generalize the above case, we first introduce a non-zero  $Z$ , the effect of which is to raise the vector  $S$ ,

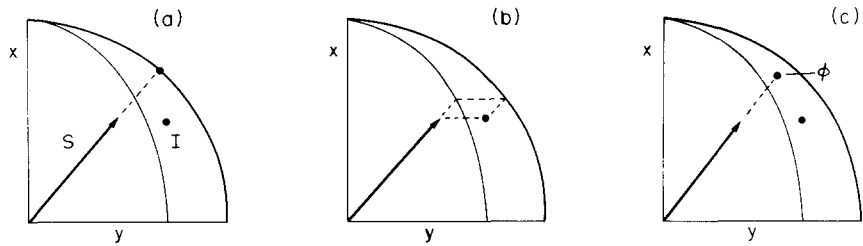


Fig. 10. (a) Orthographic construction for the special case of infinite compression along Z. (b) Construction for finding S in (a). Dashed lines are parallel to radii and latitude lines of the net. (c) Introduction of a finite stretch Z gives S a plunge  $\phi$  as determined in Fig. 11.

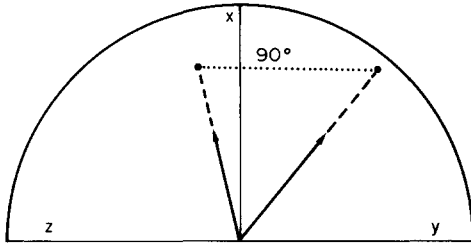


Fig. 11. Supplementary construction for determining the plunge  $\phi$  in Fig. 10(c). Fig. 10(b) is repeated for the XY- and XZ-sections. Then the plunge  $\phi$  is chosen to be consistent with a  $90^\circ$  rotation about X.

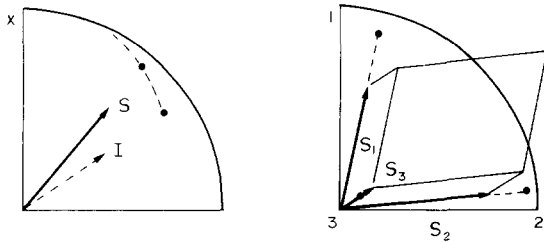


Fig. 12. (a) General construction for the case of a non-unit principal stretch X. (b) Parallelepiped representing the three-dimensional tensor S.

the deformed equivalent of  $I$ , out of the  $XY$ -plane into some general orientation of plunge  $\phi$ . The projection  $P(S)$  of  $S$  back onto the  $XY$ -plane is unaffected by the numerical value of  $Z$  but the plunge of the point where  $S$  'pierces' the unit sphere must be determined in order to distinguish  $S$  from all other vectors whose projections coincide with  $P(S)$ . This is done in Fig. 11 using a supplementary construction. For full generality, we must also permit non-unit values of  $X$  in which case the initial condition is represented, not by the sphere of which the net is a projection, but rather by a concentric sphere of radius  $\sqrt[3]{XYZ}$  (Fig. 12).

Application of the above constructions to any orthonormal triad  $I_j$  yields the column vectors  $S_j$  of the three-dimensional stretch tensor  $S$ . This tensor is represented by a projected parallelepiped in Fig. 12(b).

The stretch ellipsoid and deformation ellipsoid are indistinguishable for the special case of irrotational deformation. In general, however, it is necessary to distinguish two stretch ellipsoids associated with each rotational deformation ellipsoid (see below).

### SURFACES RELATED TO THE STRETCH ELLIPSOID

#### The displacement ellipsoid

The set of all displacement vectors  $U$ , which join points on the unit sphere to their deformed positions on the concentric stretch ellipsoid are themselves distributed on an ellipsoid, the displacement tensor's ellipsoid (Truesdell & Toupin 1960, p. 247 used the term displacement gradients tensor; Malvern 1969, p. 124 referred to the unit relative displacement matrix, alternatively named the Jacobian matrix). The tensor's column vectors may be expanded as follows,

$$U = [U_1 \quad U_2 \quad U_3] = \begin{bmatrix} \epsilon_1 & T_{12} & T_{13} \\ T_{21} & \epsilon_2 & T_{23} \\ T_{31} & T_{32} & \epsilon_3 \end{bmatrix} \quad (20)$$

Principal displacement vectors and principal extensions are equal in magnitude for irrotational deformations, but care should be taken not to confuse extensions and elongations in general.

The orthographic construction for displacement is similar to that for stretch but now the axes may differ in sign (Fig. 13). For example, if the principal extension  $U_Y$  is negative (representing a contraction) and is smaller in magnitude than  $U_X$ , the displacement of a unit vector initially at  $\theta$  to the  $X$ -direction is determined by setting off a pitch of  $-\theta$  and reading the corresponding radius of the displacement ellipse (Fig. 13b). Displacement vectors in the vicinity of  $U_X$  have outward-directed elongations while those close to  $U_Y$  are inward-directed. In two dimensions, a unique pair of directions suffers no extension in the current increment of infinitesimal deformation, representing directions which rotate without stretching. Another unique pair of directions will have suffered no cumulative extension.

For infinitesimal irrotational displacements, the approximations

$$\epsilon = e \quad (21)$$

$$T = \rho \quad (22)$$

$$|\rho_1| = |\rho_2| \quad (23)$$

$$|\rho_1| + |\rho_2| = \gamma \quad (24)$$



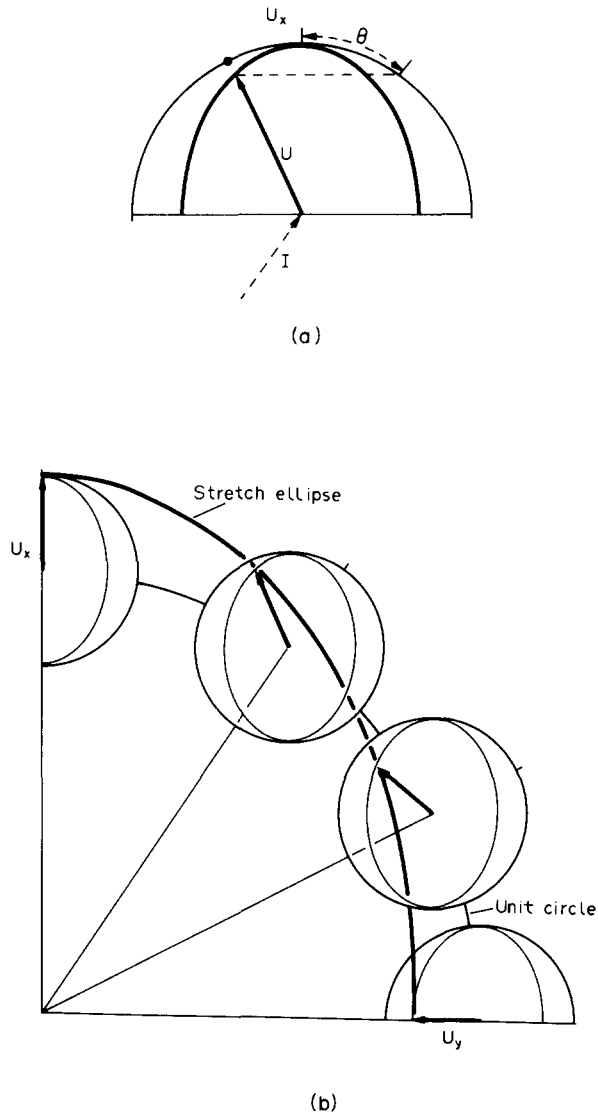


Fig. 13. (a) Orthographic construction for the displacement ellipse.  $U_x$  represents lengthening and  $U_y$  shortening.  $I$  is an arbitrary initial unit vector at  $\theta$  to the  $U_x$ -direction.  $U$  is obtained by setting off the angle  $-\theta$  on the great circle representing the displacement ellipse. Alternatively a line of latitude (dashed) may be drawn through  $+\theta$  on the perimeter and its intersection point on the ellipse recorded. (b) A set of four displacement constructions superimposed on the radii of the unit circle. The corresponding displacement vectors touch the stretch ellipse.

become valid, so that equation (20) for the two dimensional case becomes,

$$U = \begin{bmatrix} e_1 & \frac{1}{2}\gamma \\ \frac{1}{2}\gamma & e_2 \end{bmatrix}. \quad (25)$$

This tensor is here termed the infinitesimal displacement tensor. The name infinitesimal strain tensor is conventional.

For a more detailed discussion of displacement fields, the reader is referred to Ramberg (1975).

*The area stretch ellipsoid and tensor*

The area stretch  $A$  of a plane of initial pole  $I$  is hereby defined as the final area of an element of unit initial area.

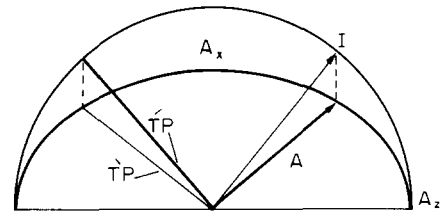


Fig. 14. Orthographic construction for the area stretch ellipse.  $A_x$  and  $A_z$  are the principal area stretch vectors.  $I$  is an arbitrary pole to a plane in the initial state. The trace of the plane is labelled  $\hat{TP}$  before deformation and  $\bar{TP}$  after.  $A$  is the area stretch vector for this plane and is perpendicular to  $\bar{TP}$ .

For the principal planes of an irrotational deformation, it is clear that we may construct a tensor

$$A = \begin{bmatrix} A_X & 0 & 0 \\ 0 & A_Y & 0 \\ 0 & 0 & A_Z \end{bmatrix} = \begin{bmatrix} YZ & 0 & 0 \\ 0 & ZX & 0 \\ 0 & 0 & XY \end{bmatrix}, \quad (26)$$

where, for example,  $A_X$  is the area stretch of the plane of initial pole  $I_X$ . If we define volume stretch  $V$  as

$$V = XYZ \quad (27)$$

then equation (26) becomes

$$A = VS^{-1}. \quad (28)$$

The tensor  $A$  is here defined as the area stretch tensor. Its ellipsoid, from equation (28), is proportional to the reciprocal stretch ellipsoid.

For irrotational deformations, the principal and reciprocal principal directions are parallel. Thus the principal area stretch vectors (the column vectors of  $A$  in diagonal form) are perpendicular to the corresponding planes before and after deformation. However, it should be clearly understood that, in the general non-diagonal case of any irrotational deformation, the column vectors of  $A$  indicate the magnitudes of the area stretches of the initial reference planes and are oriented perpendicular to those planes after deformation (Fig. 14).

*The quadratic stretch ellipsoid and tensor*

Consider the unit vector at  $\theta$  to the principal stretch vector  $X$  in the  $XY$ -plane. Choosing the principal directions as reference axes, the stretch vector for the  $\theta$ -direction may be written

$$\begin{bmatrix} X \cos \theta \\ Y \sin \theta \end{bmatrix} = \begin{bmatrix} X & 0 \\ 0 & Y \end{bmatrix} \begin{bmatrix} \cos \theta \\ \sin \theta \end{bmatrix}. \quad (29)$$

The stretch  $S$  is therefore given by Pythagoras,

$$S = \sqrt{X^2 \cos^2 \theta + Y^2 \sin^2 \theta} \quad (30)$$

or, in terms of quadratic stretch,

$$\lambda = \lambda_X \cos^2 \theta + \lambda_Y \sin^2 \theta. \quad (31)$$

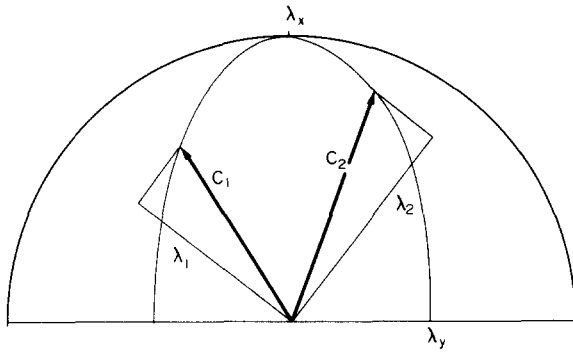


Fig. 15. Orthographic construction for the quadratic stretch ellipse. See text for full explanation.

The magnitude of the normal component  $N$  of  $S$  is given by

$$N = (X \cos \theta) \cos \theta + (Y \sin \theta) \sin \theta \quad (32)$$

or

$$N = N_X \cos^2 \theta + N_Y \sin^2 \theta \quad (33)$$

since principal stretches are entirely normal for irrotational deformations.

Equations (31) and (33) are identical in form and prompt the following analysis. Let us construct on the orthonet an ellipse with semi-axes  $\lambda_X$  and  $\lambda_Y$  (Fig. 15). These semi-axes are the principal vectors of Finger's and Green's tensors, which are indistinguishable from one another for irrotational deformation (Truesdell & Toupin 1960, p. 264). We here use the name quadratic stretch tensor and the symbol  $C$ . The columns of  $C$ , the quadratic stretch vectors  $C_j$ , exist in a quadratic reference frame, not in physical space, but their components may be expanded (Ramsay 1967, p. 71),

$$\begin{aligned} C &= [C_1 \quad C_2] \\ &= \begin{bmatrix} \lambda_1 & A_3 \gamma \\ A_3 \gamma & \lambda_2 \end{bmatrix} \end{aligned} \quad (34)$$

where  $\gamma$  is the common magnitude of the shear strains of the  $I_1$  and  $I_2$  reference vectors and  $A_3$  is the area stretch of the plane of initial pole  $I_3$ .

#### The reciprocal quadratic stretch tensor and ellipsoid

The tensor  $C$  is useful for the analysis of two-dimensional stretch at constant area but the equivalent three-dimensional form involves unknown area stretches of the reference planes and these do not vanish even when volume is conserved. The reciprocal quadratic stretch tensor  $c$  is considerably more useful,

$$c = \begin{bmatrix} \lambda_1^{-1} & \lambda_2^{-1} \gamma_2 \\ \lambda_1^{-1} \gamma_1 & \lambda_2^{-1} \end{bmatrix} \quad (35)$$

(e.g. Ramsay 1967, p. 73). Since this is a symmetric tensor

$$\gamma_1 / \gamma_2 = \lambda_1 / \lambda_2. \quad (36)$$

Note that  $\gamma_1$  and  $\gamma_2$  are the shear strains of the initial directions which become the  $I_1$  and  $I_2$ -directions after deformation. Expansion to three dimensions now involves no unknown areal factors,

$$c = \begin{bmatrix} \lambda_1^{-1} & \lambda_2^{-1} \gamma_{12} & \lambda_3^{-1} \gamma_{13} \\ \lambda_1^{-1} \gamma_{21} & \lambda_2^{-1} & \lambda_3^{-1} \gamma_{23} \\ \lambda_1^{-1} \gamma_{31} & \lambda_2^{-1} \gamma_{32} & \lambda_3^{-1} \end{bmatrix} \quad (37)$$

and all parameters refer to orthogonal reference directions in the deformed state (for example,  $\gamma_{21}$  is the component in the  $I_2$ -direction of the shear strain on the plane of final pole  $I_1$ ).

#### The classical strain tensor

It is possible to define a quadratic displacement tensor and ellipsoid, the latter being the locus of the vectors which join points on the surface of the initial unit sphere to the corresponding points on the quadratic stretch ellipsoid. Any set of conjugate radii of this quadratic displacement ellipsoid may form the columns of the quadratic displacement tensor which is here denoted  $2E$  since it is twice the magnitude of the classical strain tensor  $E$  (e.g. Truesdell & Toupin 1960, p. 266). However, there seems to be little merit in such an esoteric exercise and the use of classical strain tensors, which is widespread in the engineering literature, would appear to have served merely to render strain studies more complicated than they need be. There may be some merit in defining quadratic measures of area stretch (Truesdell & Toupin 1960, p. 263) but the linear equivalent introduced in the previous section on area stretch is arguably preferable in practice.

#### The natural strain ellipsoid and tensor

The natural strain ellipsoid is hereby defined as an ellipsoid oriented parallel to the stretch ellipsoid with semi-axes proportional to the natural logarithms of the principal stretches,  $\epsilon_X$ ,  $\epsilon_Y$  and  $\epsilon_Z$ . The ellipsoid is thus associated with the natural strain tensor  $H$  whose diagonal form is

$$H = \begin{bmatrix} \epsilon_X & 0 & 0 \\ 0 & \epsilon_Y & 0 \\ 0 & 0 & \epsilon_Z \end{bmatrix}. \quad (38)$$

It must be emphasized that natural strains, the logarithms of linear stretches, are not distributed on an ellipsoid. Only the principal natural strains are so distributed, just as, in the case of displacement, only the principal extensions are radii of the displacement ellipsoid. The remaining radii of the natural strain ellipsoid are unknown and probably complex functions of the corresponding natural strains. Truesdell & Toupin (1960, p. 259) defined the tensor  $H$  as

$$H = \frac{1}{2} \ln(C) \quad (39)$$

but gave no simple method for determining the components in a general reference frame, given the com-

ponents of *C*. Nevertheless, for the purpose of the following analysis (which was first presented to the Tectonic Studies Group A.G.M., Nottingham, 1979) it is sufficient that the natural strain tensor may be expressed in terms of its principal vectors.

The diagonalized stretch tensor *S* may be factored into an isotropic and plane component,

$$\begin{bmatrix} X & 0 & 0 \\ 0 & Y & 0 \\ 0 & 0 & Z \end{bmatrix} = \begin{bmatrix} Y & 0 & 0 \\ 0 & Y & 0 \\ 0 & 0 & Y \end{bmatrix} \begin{bmatrix} X/Y & 0 & 0 \\ 0 & 1 & 0 \\ 0 & 0 & Z/Y \end{bmatrix}. \quad (40)$$

Similarly, the natural strain tensor *H* may be expressed as the sum of an isotropic natural volume strain and a biaxial natural strain

$$\begin{bmatrix} \epsilon_X & 0 & 0 \\ 0 & \epsilon_Y & 0 \\ 0 & 0 & \epsilon_Z \end{bmatrix} = \begin{bmatrix} \epsilon_Y & 0 & 0 \\ 0 & \epsilon_Y & 0 \\ 0 & 0 & \epsilon_Y \end{bmatrix} + \begin{bmatrix} \epsilon_X - \epsilon_Y & 0 & 0 \\ 0 & 0 & 0 \\ 0 & 0 & \epsilon_Z - \epsilon_Y \end{bmatrix}. \quad (41)$$

In practice,  $\epsilon_Z - \epsilon_Y$  will be negative in value. The diagonal components of the biaxial part may be recognized as the Cartesian coordinates representing the deformation on the Flinn plot (1978). Let  $(\bar{\epsilon}, \kappa)$  be the polar coordinates, measured from the semi-minor axis of the natural strain ellipsoid, so that Flinn's parameter

$$k = \tan(\kappa). \quad (42)$$

By drawing a stereovector (De Paor 1979) of magnitude  $\bar{\epsilon}$  at an angle  $\kappa$  to the *Z*-direction in the *XZ*-plane, we combine the Flinn plot with a simple representation of the ellipsoid's orientation in space (Fig. 16). The shape of the ellipsoid is immediately evident from this diagram, since  $\kappa$  is less than 45° in the oblate field and greater than 45° in the prolate field. The point from which  $\kappa$  is measured is the pole to the *XY*-plane of the deformation.

*The structural skiodrome*

To aid analysis of the relationship between the state of deformation in three dimensions and the consequent stretch observed in an arbitrary section plane, an analogy may be drawn between the stretch ellipsoid of structural geology and the indicatrix of optical mineralogy (e.g. Wahlstrom 1951). The velocity with which a ray travels through a mineral depends upon the direction of vibration in the associated wavefront. The latter vibration may be factored into two 'permitted' components whose velocities are inversely proportional to the radii of the indicatrix to which they are parallel. These velocities may be recorded along the direction of the ray and the analysis repeated for all rays emanating from a source so as to build up a double surface called the ray velocity surface. A direct structural analogue is not appropriate because the relationship between ray velocities and refractive indices is inverse and because light rays and wavefronts are conjugate, not orthogonal. However

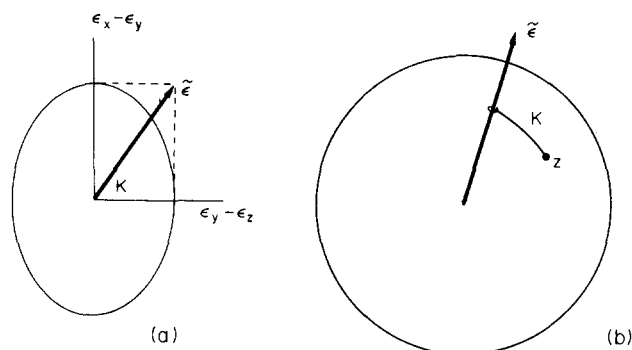


Fig. 16. (a) The natural strain ellipse's biaxial component superimposed on the deformation plot. The bold vector is the position vector of the point representing the corresponding stretch ellipsoid on the plot. Its polar coordinates are  $(\bar{\epsilon}, \kappa)$ . (b) Representation of the stretch ellipsoid on the orientation net. The stereovector is the projection of the vector in (a). *Z* is the pole to the *XY*-plane of the stretch ellipsoid.

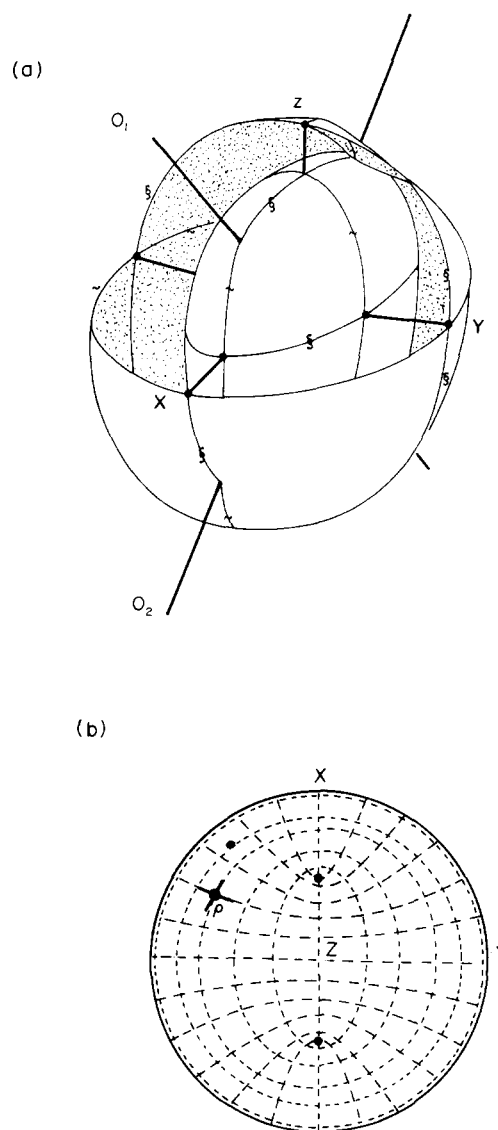


Fig. 17. (a) The sectional stretch surface with the front upper quadrant of the outer shell removed to reveal the inner shell. Bold lines mark the principal directions and the poles to the circular sections, *O*<sub>1</sub> and *O*<sub>2</sub>. The traces of the surface in the principal planes are labelled § where circular and ~ where elliptical. They all appear elliptical in this perspective. (b) The structural skiodrome, an orthographic projection of the surface in (a). *P* is the pole to a plane. The contour values at *P* give the semiaxes of the corresponding sectional stretch ellipse. The great circles which are tangent to the contours at *P* (bold cross) intersect the plane in the sectional stretching directions.

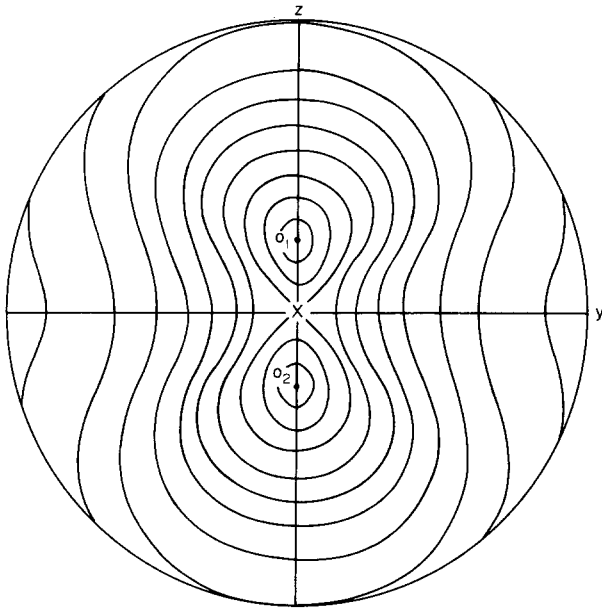


Fig. 18. Loci of equal sectional stretch ratio on the orthonet. The contours rise from unity in the 'optic axis' directions to  $X/Z$  in the  $Y$ -direction. Note the similarity to isochromatics in mineral optics.

Wahlstrom (1951) described another surface called the index surface, whose radii record the maximum and minimum refractive indices in the plane to which they are perpendicular. This surface has the same type of shape as the better known ray velocity surface; it is a double surface whose inner and outer parts touch in optic axial directions and whose principal sections comprise circles and ellipses. In the stretch ellipsoid, by analogy, the double surface will be called the sectional stretch surface (Fig. 17). The pole to an arbitrary plane cuts this surface in two lengths equal to the semi-major and semi-minor axes of the stretch ellipse in that plane. An orthographic projection of the surface is called the structural skiodrome, by an analogy with the optical skiodrome (Fig. 17) as defined by Bates & Jackson (1980, p. 586). The lines drawn on the skiodrome are contours of the sectional stretch surface and, therefore, they give the stretch data required for a plane whose pole is marked upon the orthonet. They also indicate the principal directions in this section as illustrated by the Biot–Fresnel construction of Fig. 17. By superimposing on the skiodrome a great circle of poles to section planes, the shape of an apparently folded lineation on a cylindrical fold surface may be analysed (cf. Sanderson 1974). It is seen, for example, that the most intense development of stretching lineation as indicated by boudin formation, need not coincide with the most intense expression of apparent lineation which is controlled by the sectional stretch ratio.

An analogy may be drawn also between the isochromatic surfaces of the biaxial optical figure and the distribution of axial ratios among the sectional ellipses of the deformation ellipsoid. This analogy is not complete, because interference colours depend on optical path differences, not ratios. However, the form of the loci of

equals sectional stretch ratio on the orthonet (Fig. 18) is quite similar to that of the biaxial figure (without the isogyres).

## THE DEFORMATION TENSOR AND ELLIPSOID

### *Polar decomposition*

Two types of deformation ellipsoid may be distinguished on the basis of the relationship between eigenvectors (directions of no rotation) and principal stretch vectors (maximum, minimax and minimum stretch directions). When these two sets of vectors are real and parallel to each other, they define the semi-axes of the stretch ellipsoid (Fig. 19a) which is the deformation ellipsoid for the special case of irrotational deformation. The orthographic and Mohr constructions for stretch have been described already. A 'rule-of-thumb' for the construction of the two-dimensional Mohr circle is that one column vector of the stretch tensor is rotated through  $90^\circ$  and then joined to the other. The Mohr circle is drawn on that join as diameter. Note that there are two equally valid implementations of this rule, as illustrated in Fig. 19(c) and (d) for the simple diagonalized case.

The second type of deformation ellipsoid is obtained from the unit sphere by a combination of stretch and rigid rotation. The principal vectors and eigenvectors of such a deformation do not coincide; indeed the latter vectors may be complex.

In order to treat rotational deformation as a two-dimensional phenomenon, we assume that the rotational component  $\mathbf{R}$  acts about the  $I_2$  reference axis and that the minimax stretch  $S_y$  acts along  $I_2$ . The deformation tensor may be represented by an orthographic construction (Fig. 19e) or by an 'off-axis' Mohr circle; the simple case of a diagonalized stretch component is illustrated in Figs. 19(f)–(h). Again there are two valid implementations of the above rule. Clearly, in either case, the Mohr circle is rotated about the origin by an angle  $\omega$  equal to the rigid rotation component of deformation. Means (this issue) has proposed an alternative rule which effectively produces the transpose of the above construction (i.e. its reflection in the  $45^\circ$ -direction). Using Means' approach (Fig. 19h) double angles measured clockwise on the Mohr circle correspond to single angles measured clockwise in physical space. However, a clockwise component of rigid rotation is represented by counter-clockwise deflections of the Mohr circles off their axes.

In a general reference frame in the  $XZ$ -plane, the deformation tensor  $\mathbf{D}$  may be written

$$\begin{aligned} \mathbf{D} &= [D_1 \quad D_3] \\ &= \begin{bmatrix} N_1 & T_3 \\ T_1 & N_3 \end{bmatrix}. \end{aligned} \quad (44)$$

This may be decomposed into the rigid rotation  $\mathbf{R}$

$$\mathbf{R} = \begin{bmatrix} \cos \omega & -\sin \omega \\ \sin \omega & \cos \omega \end{bmatrix} \quad (45)$$

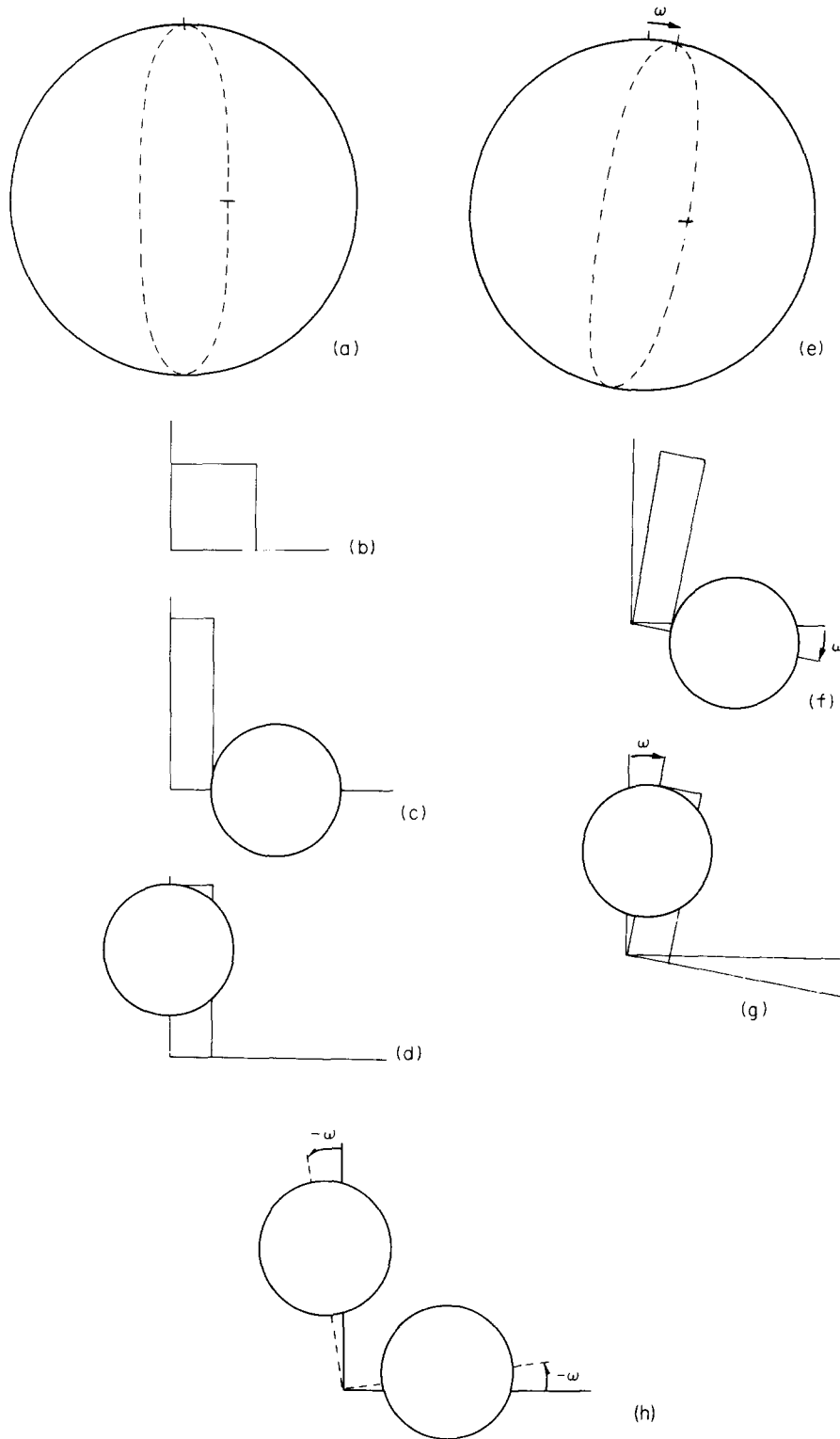


Fig. 19. (a) Orthographic construction for irrotational stretch. The tick marks indicate the stretched lengths of the sides of the square in (b). (c) Mohr circle for stretch obtained from the principal stretch vectors (the sides of the rectangle in this case). The long side of the rectangle is rotated through  $90^\circ$  and then joined to the short, the Mohr circle being constructed on this join. (d) An alternative construction to (c). Here, the short side of the rectangle has been rotated while the long side remains fixed. (e) Orthographic construction for stretch and rotation through an angle  $\omega$ . The tick marks again represent the stretch vectors for the sides of the square in (b). (f) Mohr circle constructed as in (c). (g) Mohr construction as in (d). (h) Means' convention (this issue) for determining the attitude of the Mohr circle (see text).

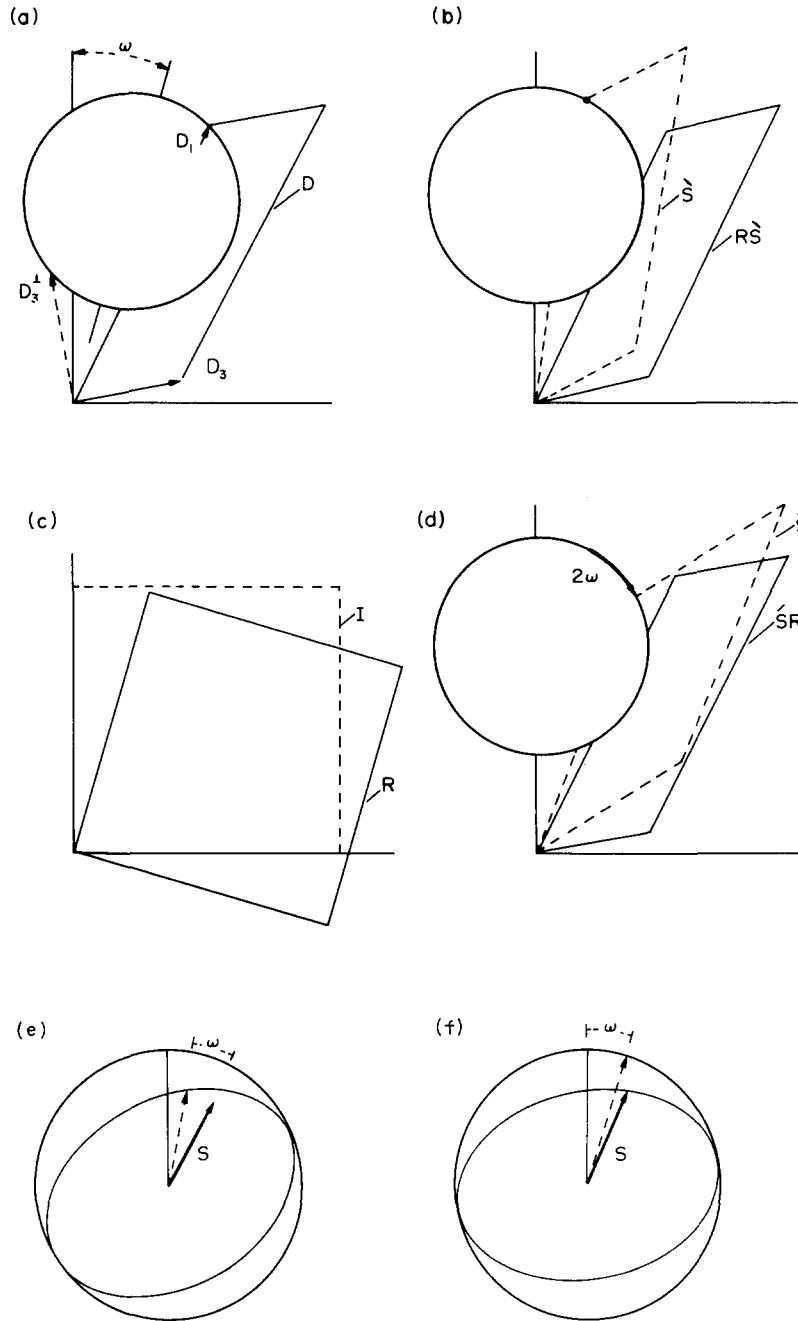


Fig. 20. (a) Mohr circle for the deformation tensor in a general reference frame, drawn as in Fig. 19(c). The circle's central axis (short line) is at  $\omega$  to the reference axis. (b) Removal of the rotational component from (a) yields the Mohr circle for the right stretch tensor (dashed parallelogram). (c) Application of the rotational component  $\omega$  to the initial unit square yields the tensor  $\mathbf{R}$ . (d) Application of the left stretch tensor (dashed parallelogram) to the tensor  $\mathbf{R}$  of (c) yields the deformation tensor  $\mathbf{SR}$  (solid parallelogram). The left stretch tensor shares the Mohr circle of (b) but touches it at a point  $2\omega$  clockwise (bold arc). (e) Orthographic construction for right polar decomposition. The arbitrary initial direction (light line) is first stretched (dashed line) and then rotated to  $\mathbf{S}$ . (f) Left polar decomposition corresponding to (e). The initial line is first rotated through  $\omega$  and then stretched to  $\mathbf{S}$ .

followed by (i.e. premultiplied by) the left stretch tensor  $\hat{\mathbf{S}}$

$$\mathbf{D} = \hat{\mathbf{S}}\mathbf{R}. \tag{46}$$

This decomposition is best illustrated on a Mohr diagram (Fig. 20). First the deformation vector  $\mathbf{D}_3^+$  is rotated to the new position  $\mathbf{D}_3^-$  with coordinates  $(-T_3, N_3)$ . Then the Mohr circle is constructed so that  $\mathbf{D}_3^-$  and  $\mathbf{D}_1$  are diametrically opposite. The rigid rotation is represented by the positive clockwise deflection of the Mohr circle

from the  $\mathbf{I}_1$  reference axis. Thus,  $\omega$  may be calculated from the ratio of the coordinates of the circle's centre,

$$\tan \omega = \frac{T_1 - T_3}{N_1 + N_3}. \tag{47}$$

The components of  $\hat{\mathbf{S}}$  are obtained by projecting  $\mathbf{D}_1$  and  $\mathbf{D}_3^+$  onto a central axis of the Mohr circle, which is equivalent to solving

$$\hat{\mathbf{S}} = \mathbf{D}\mathbf{R}^t. \tag{48}$$

As an alternative to the left-polar decomposition described above, the tensor may be decomposed into the same rotation  $\mathbf{R}$  postmultiplied (i.e. preceded) by the right stretch tensor  $\hat{\mathbf{S}}$ ,

$$\mathbf{D} = \mathbf{R}\hat{\mathbf{S}}. \quad (49)$$

Comparing equations (48) and (49), it is clear that

$$\hat{\mathbf{S}} = \mathbf{R}\hat{\mathbf{S}}\mathbf{R}^t. \quad (50)$$

Thus, the right stretch and left stretch ellipses are identical in shape and the difference in their orientations equals the rotational component of deformation (Fig. 20). The right stretch ellipse has the same shape as the deformation ellipse but its axes in ascending order parallel the axes in descending order of the reciprocal deformation ellipse. The left stretch ellipse has the shape and orientation of the deformation ellipse but differs in the locations of material points on the elliptical outline. A rigid rotation of the unit circle must be applied first, in order to obtain congruence with the deformation ellipse.

Having determined the above decompositions, two orthographic constructions may be employed for the analysis of rotational deformations (Figs. 20e and f). These apply to any rotational deformation. However, the special case of simple shear deserves to be considered more fully. This is done in the next section.

### Simple shear

We define simple shear deformation as

$$\begin{aligned} \mathbf{D} &= [D_a \quad D_c] \\ &= \begin{bmatrix} 1 & \gamma \\ 0 & 1 \end{bmatrix} \end{aligned} \quad (51)$$

where  $\mathbf{a}$  is the tectonic transport direction and  $\mathbf{c}$  is the pole to the shear plane. The symbols  $\mathbf{a}$ ,  $\mathbf{c}$  and the format  $\mathbf{a}$ -horizontal,  $\mathbf{c}$ -vertical are rooted in the geological literature and so are preferred to 1, 3 in this case. Ramsay & Graham (1970) measured angles both clockwise of  $\mathbf{c}$  and counterclockwise of  $\mathbf{a}$ ; in this paper all angles are measured clockwise of  $\mathbf{c}$ . In Fig. 21(a), a line is drawn at a relative hade of  $\omega$ . Clearly this material line was initially at  $-\omega$  and is a line of unit stretch. Of course, the second direction of unit stretch coincides with  $\mathbf{a}$ . The obtuse angle  $2V_0$  between the initial unit stretch directions becomes an acute angle  $2V$  after deformation and the acute initial angle,  $2V$  becomes numerically equal to  $2V_0$ . The initial (right) and final (left) principal stretch directions must bisect  $2V_0$  and  $2V$ , respectively; therefore

$$\begin{aligned} V_0 &= 45^\circ + \omega/2 \\ V &= 45^\circ - \omega/2. \end{aligned} \quad (52)$$

Thus, the initial semi-major axis lies at a hade of  $V$  and is rotated through  $\omega$  to an attitude  $V_0$ . Since the stretch component of deformation does not rotate the principal directions,  $\omega$  must be the rigid rotation component. Therefore, equations (45) and (48) yield

$$\begin{aligned} \mathbf{D} &= \hat{\mathbf{S}}\mathbf{R} \\ &= \begin{bmatrix} \cos \omega + \gamma \sin \omega & \sin \omega \\ \sin \omega & \cos \omega \end{bmatrix} \begin{bmatrix} \cos \omega & \sin \omega \\ -\sin \omega & \cos \omega \end{bmatrix} \end{aligned} \quad (54)$$

while equations (45) and (50) yield

$$\begin{aligned} \mathbf{D} &= \mathbf{R}\hat{\mathbf{S}} \\ &= \begin{bmatrix} \cos \omega & \sin \omega \\ -\sin \omega & \cos \omega \end{bmatrix} \begin{bmatrix} \cos \omega & \sin \omega \\ \sin \omega & \cos \omega + \gamma \sin \omega \end{bmatrix}. \end{aligned} \quad (55)$$

The Mohr construction for simple shear (Fig. 21b) may be used to determine the stretches and rotations of arbitrary directions in the initial or final state but care must be taken to employ the correct sign convention. Thus, the stretch  $S$  and rotation  $\alpha$  of a direction of initial hade  $\theta$  are obtained from the polar coordinates of a point  $2\theta$  counterclockwise of the Cartesian point  $(\gamma, 1)$  on the Mohr circle. An expression for the stretch follows from the geometry of the figure,

$$S = \sqrt{\sec^2 \omega + \tan^2 \omega + 2 \sec \omega \tan \omega \cos 2(V - \theta)}. \quad (56)$$

The orientation of the corresponding direction after deformation is  $\arctan(\tan \theta + \gamma)$  (Ramsay 1967, p. 88). The reciprocal deformation ellipse, tensor and Mohr circle are obtained by reflection in the  $\mathbf{c}$ -axis. Therefore, the reciprocal stretch  $S^{-1}$  of a direction of final hade  $\theta$  is obtained by setting off  $2\theta$  clockwise from  $(\gamma, 1)$  on the Mohr circle of Fig. 21(b).

The principal stretch vectors of simple shear deformation,  $\mathbf{X}$  and  $\mathbf{Z}$  may be derived from a dyadic circle (Durelli *et al.* 1958), a circle concentric with the Mohr circle but passing through the origin (Fig. 21c). The intersections of a horizontal line through  $(0, 1)$  with the dyadic circle define the principal stretches as follows,

$$\begin{aligned} X &= \tan V_0 \\ Z &= \tan V \end{aligned} \quad (57)$$

(see Thompson & Tait 1867, Treagus 1981). Thus, the polar coordinates of the semi-major stretch  $X$  for example, may be written  $(\tan V_0, V_0)$ .

The eigenvectors of simple-shear deformation coincide with the  $\mathbf{a}$ -axis, as indicated by the tangency of the Mohr circle to the  $\mathbf{c}$ -axis. This reflects the fact that in simple shear, there is really only one direction of no rotation in the  $\mathbf{XZ}$ -plane and that is the direction of the  $\mathbf{a}$ -axis. In any plane other than the  $\mathbf{XZ}$ -plane, simple shear will resemble transpression or transtension, depending on the sign of the area stretch. Thus, the critical feature of simple shear in general is the coincidence of the eigenvectors with the shear plane.

### Classification of rotational deformations

So far, we have discussed three special cases of deformation: pure shear, simple shear and rigid rotation.

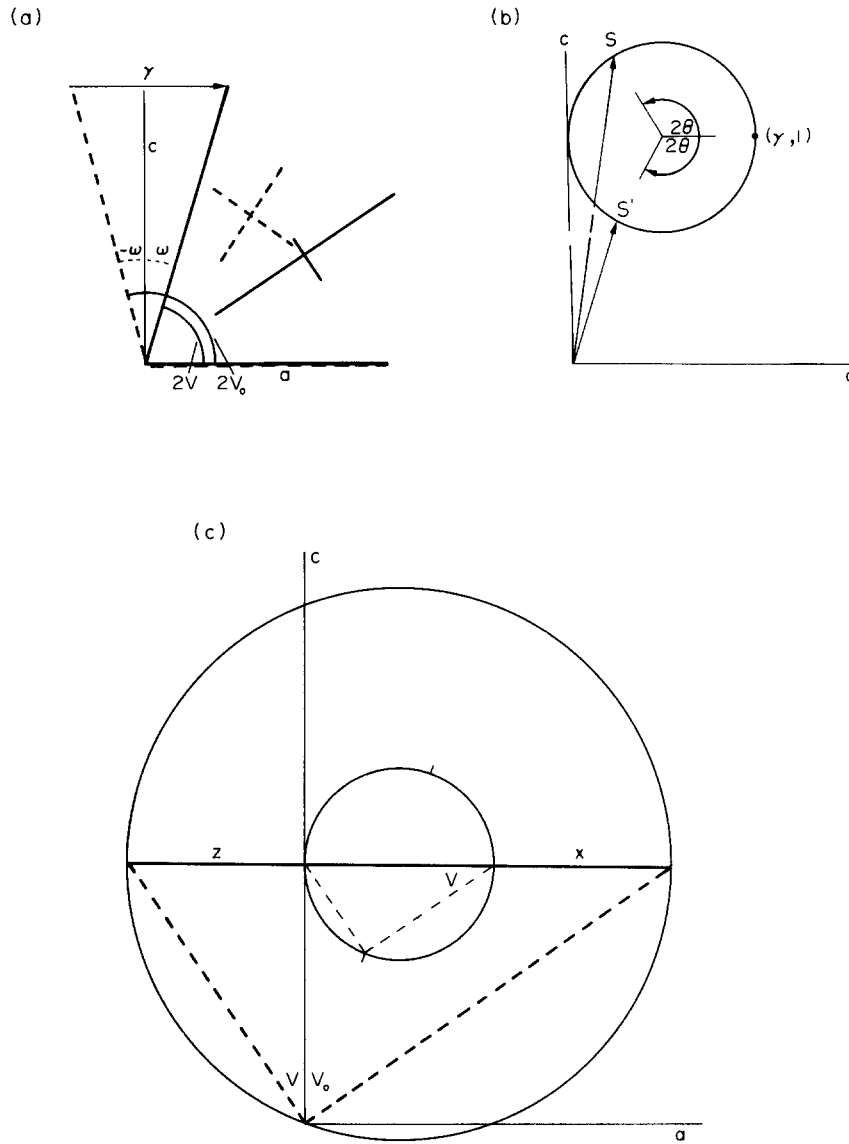


Fig. 21. Geometric features of simple shear. (a)  $a$  is the shear direction and  $c$  the pole to the shear plane.  $2V_0$  is the initial obtuse angle between the circular sections of the deformation ellipsoid and  $2V$  is its deformed equivalent. The dashed and solid crosses represent the initial and final principal stretch directions. The Mohr circle for simple shear (b) touches the  $c$ -axis.  $S$  is the stretch of an arbitrary direction initially at  $\theta$  to the  $c$ -axis.  $S'$  is the reciprocal stretch of the direction finally at  $\theta$  to  $c$ . The dyadic circle for simple shear (c) is concentric with the Mohr circle but passes through the origin. Its inscribed right-angled triangle defines the principal directions and its hypotenuse is divided by the  $c$ -axis into lengths  $X$  and  $Z$ . These geometric features follow from the corresponding features of the Mohr circle as shown.

These may be considered end-members of a continuous series of plane deformations of which five types may be labelled pure shear, sub-simple shear, simple shear, super-simple shear and rigid rotation (Fig. 22). Note that this classification is entirely independent of the statistics of Matthews *et al.* (1974), but is consistent with the classifications of Ramberg (1975) and Means *et al.* (1980).

For consistency, the Mohr circle for pure shear is centred on the vertical axis in Fig. 22. The sub-simple shear circle cuts that axis in two points representing two real but non-orthogonal eigenvectors in the  $XZ$ -plane. Points counterclockwise of the vertical represent directions which have suffered counterclockwise rotation in the physical plane. The simple shear case is the boundary

between such sub-simple shears and the class of super-simple shears, shears involving more rotation than is appropriate to simple shear. The eigenvectors in the  $XZ$ -plane of super-simple shear are complex since all lines really suffer some rotation.

If the final state of finite deformation is achieved by identical increments of displacement, the five classes of deformation will be clearly distinguished by their zones of lengthened–shortened radii (Ramsay 1967, p. 114). It should be noted that superposed pure shears with different  $X$ -directions always yield a net sub-simple shear while superimposed simple shears of the same sense, with different  $a$ -directions always produce net super-simple shear. Also, a pure shear acting across the plane of simple shear is equivalent to a sub-simple shear.



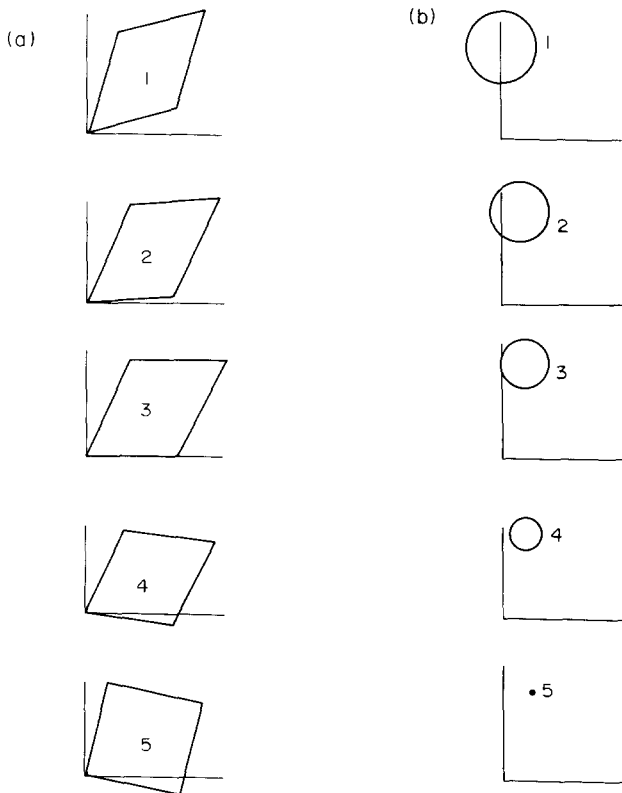


Fig. 22. The five classes of rotational deformation represented by tensors (a) and Mohr circles (b).

As an example of the application of the above theory, D. Sanderson (pers. comm.) has suggested considering the state of deformation in the hanging wall of a thrust sheet as it encounters a ramp. As the sheet begins to climb the ramp, the state of deformation may be expected to change from pure shear to sub-simple shear to simple shear. Then as the sheet mounts the top of the ramp, the rotational component of deformation may increase till super-simple shear is achieved. Thus, an early slaty cleavage developed during the climb may become crenulated when it passes from the zone of lengthening into the zone of shortening. As a second example, a combination of sub-simple and super-simple shear may achieve compatibility at a ductile shear zone termination (D. Sanderson, pers. comm.).

### Three-dimensional analysis

Relative to an arbitrary reference frame  $\mathbf{I}$  the three-dimensional deformation tensor may be written

$$\mathbf{D} = [D_1 \ D_2 \ D_3]. \quad (58)$$

This may be subject to left or right polar decomposition, an orthographic construction for both of which is illustrated in Fig. 23. In order to display the rotational component of deformation, the surface of the initial sphere was marked with lines of latitude and longitude. These were first rotated into an oblique orientation by application of the tensor  $\mathbf{R}$ . Then the graticule was stretched into the shape of the left stretch ellipsoid. The same net effect would have been achieved by applying

the right stretch ellipsoid to the  $\mathbf{R}^t$ -directions and then applying the tensor  $\mathbf{R}$  to the resultant graticule. The construction may be used to determine the deformed state of an arbitrary initial direction by applying the rotation using standard orientation net techniques and then treating the problem as for stretch (of course, the graticule of latitude and longitude lines need not be drawn in practice).

The orthographic construction for simple shear in three dimensions is particularly elegant (Fig. 24a). The pole to the shear plane  $c$  is aligned with the north axis of the net so that the shear plane contains east–west and up–down. It must be clearly understood, therefore, that the construction represents the simple shear deformation ellipsoid viewed along the tectonic transport direction  $a$  (the above usage of ‘north’, etc. will not be continued, as the geographic poles may plot anywhere on the net). Viewed in this direction, the deformation ellipsoid always looks like a projected sphere because all displacement vectors are parallel to the orthographic projection vectors! Furthermore, if the net axis is aligned perpendicular to the  $ac$ -plane, the axis and great circle representing a tilt of  $\pm\omega$  define the ellipsoid’s circular sections before and after deformation. To determine the deformed state of an arbitrary initial plane (Skjernaa 1980) its lines of intersection with the circular sections should be noted. One such line will lie in the shear plane and be unaffected by the deformation. The other will simply move from being represented by a point on the back hemisphere to a congruent position on the front hemisphere or vice versa (Fig. 24b). The deformed plane is fitted to these two deformed lines. To determine the deformed state of an arbitrary initial line we draw the great circle containing it and the  $c$ -axis and the great circle containing it and the  $a$ -axis. After deformation these two planes intersect in the direction of the required deformed line (Fig. 24c). It is noticed that the attitudes of all lines converge on the  $a$ -axis. Poles to deformed planes act in an inverse manner (Owens 1973), converging on the  $c$ -axis. By applying equal increments of simple shear to a grid of lines or poles, a net may be constructed which will permit rapid analysis of the effects of simple shear upon fabric elements (see also Ramsay 1980, Skjernaa 1980, Treagus & Treagus 1981).

Orthographic analysis of sub-simple and super-simple shear deformations in three dimensions may be approached similarly, by aligning the net axis with the minimax stretch and recording the attitudes of the circular sections before and after deformation.

### Additive decomposition

The deformation tensor may be decomposed into a symmetric and skew-symmetric part as follows,

$$\mathbf{D} = \tilde{\mathbf{S}} + \tilde{\mathbf{R}} \quad (59)$$

where  $\tilde{\mathbf{R}}$  is what Truesdell & Toupin termed the mean rotation tensor of Cauchy and Novozhilov (Truesdell & Toupin 1960, p. 275) and  $\tilde{\mathbf{S}}$  is here termed the additional stretch. Ramsay (1967, p. 124) wrongly suggested that  $\tilde{\mathbf{S}}$

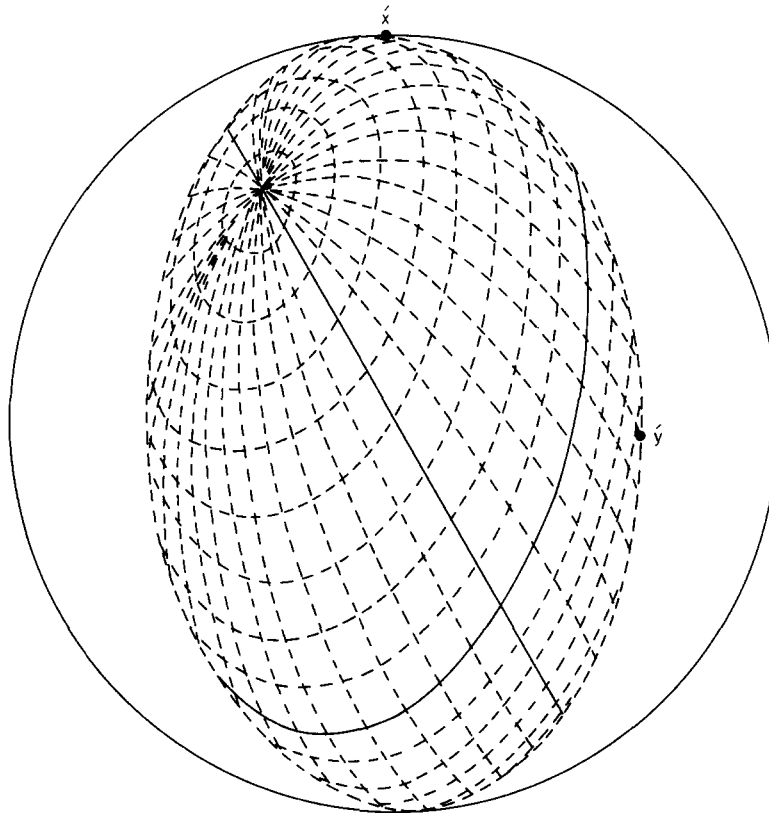


Fig. 23. Orthographic construction for three dimensional deformation (hand-drawn). Solid arcs were initially vertical-north and vertical-east.  $X$  and  $Y$  are eigenvectors of the left stretch tensor.

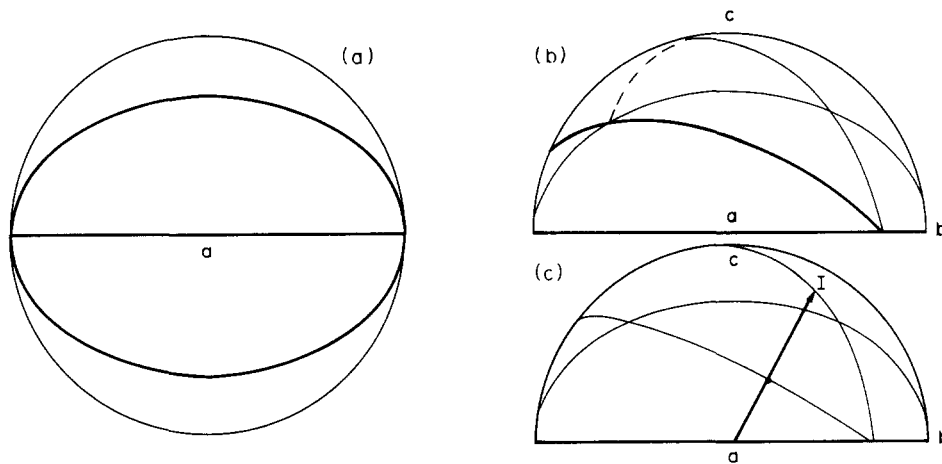


Fig. 24. Orthographic construction for simple shear in three dimensions. (a) Shear plane is horizontal and  $a$  is directed towards the viewer above the shear plane. The great circles shown are the circular sections of the deformation ellipsoid. (b) Determination of the deformation of an arbitrary plane (light arc dashed on back hemisphere). The deformed plane is shown bold. (c) Determination of the deformation of an arbitrary line by considering it as the line of intersection of two planes, one containing  $c$ , the other containing  $a$ .

was analogous to  $\hat{S}$ .  $\hat{S}$  may be further subdivided as follows

$$\hat{S} = \mathbf{I} + \hat{E}, \quad (60)$$

where  $\hat{E}$  is the elongation tensor of Truesdell & Toupin (1960, p. 266). The tensor  $\hat{R}$  is best understood from the special case where the elongation tensor is void (Fig. 25a) so that

$$\mathbf{D} = \mathbf{I} + \hat{R}. \quad (61)$$

Clearly the effect of this deformation is to rotate the initial unit square and magnify it isotropically (a two dimensional view suffices). Therefore,  $\hat{R}$  should logically be called a magnified rigid displacement tensor, since its column vectors are the displacement vectors of the reference axes. The effects of the additional stretch tensor  $\hat{S}$  must be added to the magnifying effects of  $\hat{R}$ . Therefore,  $\hat{S}$  is coaxial with  $\hat{S}$  but produces different principal stretch ratios. Prior to the invention of off-axis

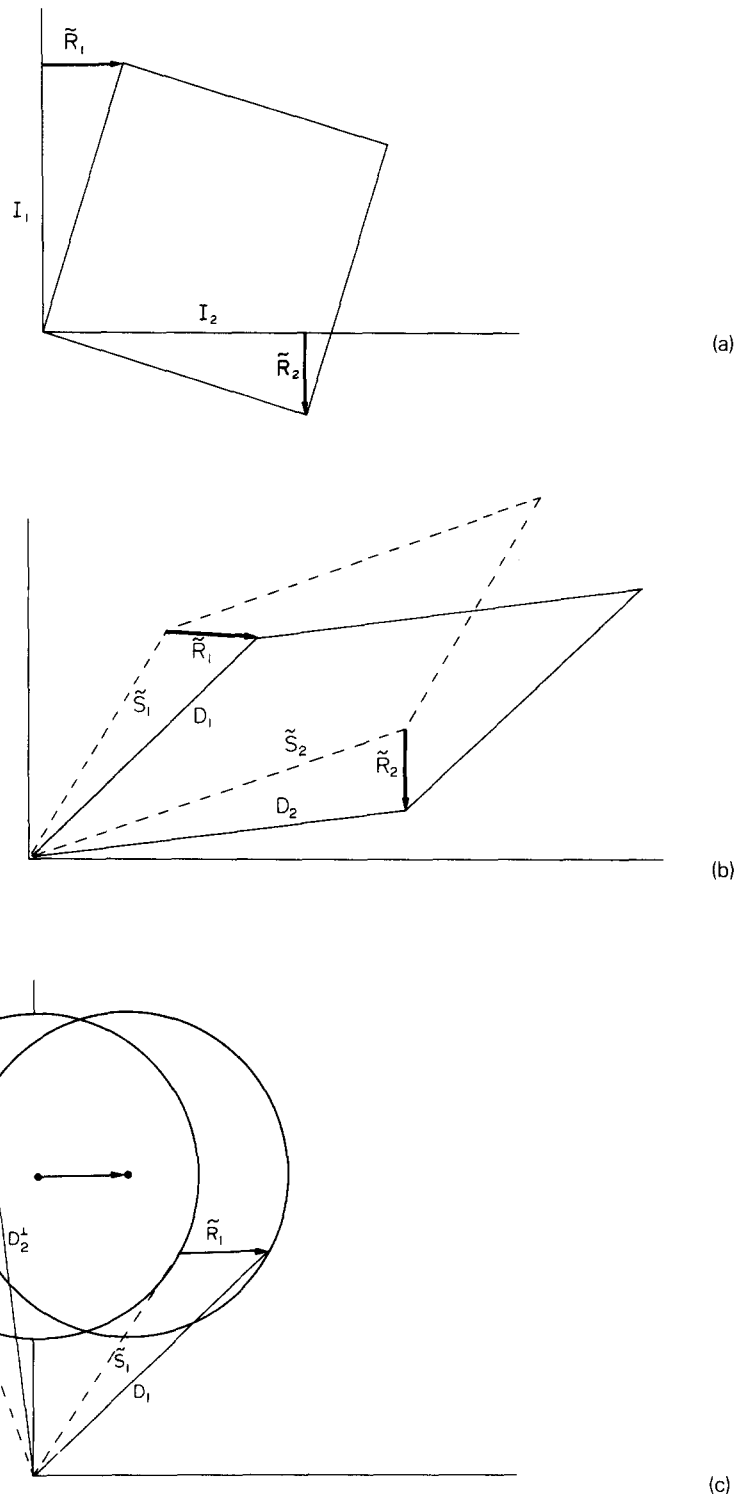


Fig. 25. (a) The effect of the tensor  $\tilde{\mathbf{R}}$  upon  $\mathbf{I}$  in the absence of any elongation  $\tilde{\mathbf{E}}$ , see text. (b) Geometric interpretation of additive decomposition. Bold arrows represent the column vectors of  $\tilde{\mathbf{R}}$ . The order of application of tensors is immaterial. (c) Mohr construction for additive decomposition. One column vector of each tensor in (b) has been rotated through  $90^\circ$  in accordance with the 'rule-of-thumb' (see text).

Mohr circles, equation (59) provided the simplest method of calculating the rotational component of deformation.

A geometric interpretation of additive decomposition is presented in Fig. 25(b). Applying the rule-of-thumb for the construction of Mohr circles to this figure yields the Mohr construction for additive decomposition (Fig.

25c) (see also Prager 1961, p. 69, Robin 1977, Lister & Williams 1983, Means this issue).

*Tensors related to the deformation tensor*

In the case of irrotational deformation, we defined the quadratic stretch tensor

$$\mathbf{C} = \mathbf{S}^2. \tag{62}$$

The symbol on the right has meaning only for a symmetric tensor. For asymmetric tensors representing rotational states of deformation, there are two ways of ‘squaring’

$$\begin{aligned} \dot{\mathbf{C}} &= \mathbf{D}\mathbf{D}^t \\ &= \dot{\mathbf{S}}\mathbf{R}\mathbf{R}^t\dot{\mathbf{S}}^t \\ &= \dot{\mathbf{S}}^2 \end{aligned} \tag{63}$$

and

$$\begin{aligned} \dot{\mathbf{C}} &= \mathbf{D}^t\mathbf{D} \\ &= \dot{\mathbf{S}}^t\mathbf{R}\mathbf{R}\dot{\mathbf{S}} \\ &= \dot{\mathbf{S}}^2. \end{aligned} \tag{64}$$

These left and right quadratic stretch tensors are commonly called Finger’s and Green’s tensors (e.g. Malvern 1969, Fung 1977). Similarly, we may take the product moments of the reciprocal deformation tensor  $\mathbf{D}^{-1}$ ,

$$\begin{aligned} \dot{\mathbf{c}} &= \mathbf{D}^{-1}\mathbf{D}^{-1} \\ &= (\mathbf{D}^t\mathbf{D})^{-1} \\ &= \dot{\mathbf{C}}^{-1} \end{aligned} \tag{65}$$

and

$$\begin{aligned} \dot{\mathbf{c}} &= \mathbf{D}^{-t}\mathbf{D}^{-1} \\ &= (\mathbf{D}\mathbf{D}^t)^{-1} \\ &= \dot{\mathbf{C}}^{-1}. \end{aligned} \tag{66}$$

These left and right reciprocal quadratic stretch tensors are commonly called Piola’s and Cauchy’s, respectively. Confusion is avoided if one remembers the tensor rule: *the reciprocal of a right tensor is a left reciprocal tensor, and vice versa.*

By way of illustration, consider again the two-dimensional simple shear

$$\mathbf{D} = \begin{bmatrix} 1 & \gamma \\ 0 & 1 \end{bmatrix}. \tag{67}$$

The reciprocal tensor is

$$\mathbf{D}^{-1} = \begin{bmatrix} 1 & -\gamma \\ 0 & 1 \end{bmatrix}. \tag{68}$$

Finger’s tensor is

$$\dot{\mathbf{C}} = \begin{bmatrix} 1 + \gamma^2 & \gamma \\ \gamma & 1 \end{bmatrix}. \tag{69}$$

Green’s tensor is

$$\dot{\mathbf{C}} = \begin{bmatrix} 1 & \gamma \\ \gamma & 1 + \gamma^2 \end{bmatrix}. \tag{70}$$

Piola’s tensor is

$$\dot{\mathbf{c}} = \begin{bmatrix} 1 + \gamma^2 & -\gamma \\ -\gamma & 1 \end{bmatrix}. \tag{71}$$

Cauchy’s tensor is

$$\dot{\mathbf{c}} = \begin{bmatrix} 1 & -\gamma \\ -\gamma & 1 + \gamma^2 \end{bmatrix}. \tag{72}$$

The function of the above set of four tensors is to isolate the irrotational component of deformation in three

dimensions; the rotational component follows from equation (46).

*Triple decomposition*

The polar or additive decomposition of deformation is unsatisfactory in practice because it is extremely difficult to form a real concept of the magnitude, *k*-value and orientation of a deformation from such components except in special cases. The following triple decomposition provides results in easily readable format.

Given the deformation tensor  $\mathbf{D}$ , Finger’s tensor  $\dot{\mathbf{C}}$  is first formed using equation (63). Its eigenvectors define the left (final) principal directions and its eigenvalues are the principal quadratic stretches. The eigenvalues are obtained first by solving the cubic characteristic equation of Finger’s tensor

$$\lambda^3 - I\lambda^2 + II\lambda - III = 0 \tag{73}$$

where I, II and III are the invariants of  $\dot{\mathbf{C}}$ . The three solutions are

$$\begin{aligned} \lambda_i &= \frac{I}{3} + \frac{2}{3} \sqrt{I^2 - 3II} \cdot \cos \frac{1}{3} \\ &\times \left[ \cos^{-1} \left[ \frac{-27III + 9I \cdot II - 2I^3}{2\sqrt{(I^2 - 3II)^3}} \right] + 2\pi(i - 1) \right], \\ & i = 1, 2, 3. \end{aligned} \tag{74}$$

Equation (74) follows from Ramsay (1967, eqn. 4–8).

By definition, when an eigenvector is premultiplied by its tensor, it is stretched but not rotated. The outcome is as if the eigenvector had been multiplied by a scalar, its eigenvalue. Having obtained the eigenvalues of  $\dot{\mathbf{C}}$  from equation (74), the corresponding eigenvectors  $\dot{\mathbf{O}}$  are obtained by solving

$$\dot{\mathbf{C}}\dot{\mathbf{O}} = \lambda\dot{\mathbf{O}} \tag{75}$$

for each scalar component of  $\dot{\mathbf{O}}$  at a time, and for each eigenvalue. Since the eigenvalues of  $\dot{\mathbf{C}}$  are equal to those of  $\dot{\mathbf{C}}$  the eigenvectors of  $\dot{\mathbf{C}}$  follow by solving

$$\dot{\mathbf{C}}\dot{\mathbf{O}} = \lambda\dot{\mathbf{O}}. \tag{76}$$

The set of eigenvectors  $\dot{\mathbf{O}}_j$ , ( $j = 1, 2, 3$ ) are placed in the columns of a tensor  $\dot{\mathbf{O}}$  and the set  $\dot{\mathbf{O}}_j$  in the columns of the tensor  $\dot{\mathbf{O}}$  (equations (75) and (76) give the eigenvectors to within a scalar factor; therefore care must be taken to set the magnitude of each to unity). Finally, the principal stretches are placed in the columns of a diagonal tensor  $\mathbf{X}$ , in corresponding order, for example,

$$\mathbf{X} = \begin{bmatrix} X & 0 & 0 \\ 0 & Y & 0 \\ 0 & 0 & Z \end{bmatrix}, \tag{77}$$

where each principal stretch is the square root of the corresponding eigenvalue  $\lambda$ . Now the deformation tensor  $\mathbf{D}$  may be expressed as the product of three components,

$$\mathbf{D} = \dot{\mathbf{O}}\mathbf{X}\dot{\mathbf{O}}^t \tag{78}$$

where  $\hat{\mathbf{O}}^1$  rotates the initial principal directions into the arbitrary reference frame,  $\mathbf{X}$  stretches the reference directions and  $\mathbf{O}$  rotates the reference directions into the final principal directions. Note that the rotational component of deformation is given by

$$\mathbf{R} = \hat{\mathbf{O}}\hat{\mathbf{O}}^1. \tag{79}$$

Equation (78) enables one to visualize immediately the intensity and  $k$ -value of a deformation, but the attitude of the principal directions must be deciphered from the direction cosines. Furthermore, there are 27 elements in the triple decomposition whereas only nine are independent. It is more meaningful to express the left and right principal directions in terms of their Euler angles, namely the strike and dip of the  $XY$ -plane and the pitch of the  $X$ -axis,  $\sigma$ ,  $\delta$  and  $\psi$ , respectively,

$$\begin{aligned} \sigma &= \arctan(O_{13}/O_{23}) \\ \delta &= \arccos(O_{33}) \\ \psi &= \arcsin(O_{31}/\sin \delta). \end{aligned} \tag{80}$$

Now the deformation recorded by the tensor  $\mathbf{D}$  may be summarized in a deformation matrix  $\mathbf{D}^*$  (not a tensor),

$$\mathbf{D}^* = \begin{bmatrix} \acute{\sigma} & X & \acute{\delta} \\ \acute{\delta} & Y & \acute{\delta} \\ \acute{\psi} & Z & \acute{\psi} \end{bmatrix} \tag{81}$$

where the left-hand column records the attitude of the final principal axes, the central column records the principal stretches and the right-hand column records the initial attitudes of the final principal axes.

### HETEROGENEOUS DEFORMATION

#### Rank-3 tensors

Hitherto we have employed rank-1 tensors (vectors) such as  $\mathbf{V}$  and rank-2 tensors (tensors) such as  $\mathbf{V}$ . A rank-3 tensor  $\mathbf{V}$  may be thought of as a row matrix, each element of which is itself a tensor,

$$\mathbf{V} = [\mathbf{V}_1 \quad \mathbf{V}_2 \quad \mathbf{V}_3]. \tag{82}$$

A rank-3 tensor transforms an input vector into an output tensor. If the input vector is the position vector of a particular location in a heterogeneous tensor field, then the corresponding output tensor may describe the state of the field at that location, provided the field is sufficiently simple and continuous to be described by the rank-3 tensor. Note that a zero input vector yields a zero output tensor regardless of the values in the rank-3 tensor. Therefore, rank-3 tensors are suitable only for the description of tensor fields which are zero-valued at the origin.

#### Heterogeneous displacement fields

At any point in a heterogeneous deformation field, the state of deformation may be factored into parts here termed the inhomogeneous part, which generally varies from location to location and an additional homo-

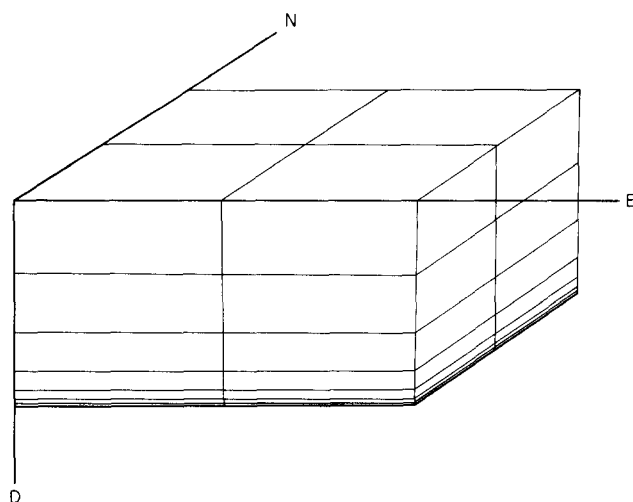


Fig. 26. A heterogeneous deformation field produced by application of rank-3 tensor algebra as discussed in the text. Only the part of the field below the horizon is shown as the rank-3 operation produces volume-gain above the surface.

geneous deformation which is everywhere equal to the state of deformation at the origin, and which is superimposed on (i.e. premultiplies) the inhomogeneous part. This factorization is entirely arbitrary and dependent on the choice of origin.

The inhomogeneous part of a heterogeneous deformation field as defined above may be further subdivided at any point into the sum of an identity tensor  $\mathbf{I}$  and a displacement tensor, the latter being zero-valued at the origin,

$$\mathbf{D} = \mathbf{U} + \mathbf{I}. \tag{83}$$

Let  $\mathbf{U}_1$ ,  $\mathbf{U}_2$  and  $\mathbf{U}_3$  be the displacement tensors at the locations  $I_1$ ,  $I_2$  and  $I_3$ , respectively. Then, if the displacement state gradients are constants, the state of displacement  $\mathbf{U}$  at an arbitrary location  $\mathbf{P}$  is given by

$$\mathbf{U} = [\mathbf{U}_1 \quad \mathbf{U}_2 \quad \mathbf{U}_3]\mathbf{P}. \tag{84}$$

The deformation state is then given by  $\mathbf{D}^{\mathbf{A}}(\mathbf{U} + \mathbf{I})$ , where  $\mathbf{D}^{\mathbf{A}}$  is the additional homogeneous deformation.

The use of rank-3 tensors for the description of heterogeneous states of deformation does not appear to have been proposed before, although Hobbs (1971) has made analogous use of rank-2 tensors with variable elements. The method proposed here is preferred because the true 'displacement gradients' are displayed in the rank-3 tensor array and because common geological strain patterns may be described by very simple rank-3 tensors. For example, the rank-3 tensor

$$\begin{bmatrix} 0 & 0 & 0 & | & 0 & 0 & 0 & | & 0 & 0 & 0 \\ 0 & 0 & 0 & | & 0 & 0 & 0 & | & 0 & 0 & 0 \\ 0 & 0 & 0 & | & 0 & 0 & 0 & | & 0 & 0 & -1 \end{bmatrix}$$

produces a field of differential compaction (Fig. 26), when north-east-down is the chosen reference frame. Displacement state gradients are zero in the horizon and constant in the vertical direction. Volume expansion is recorded above the horizon while infinite compaction is

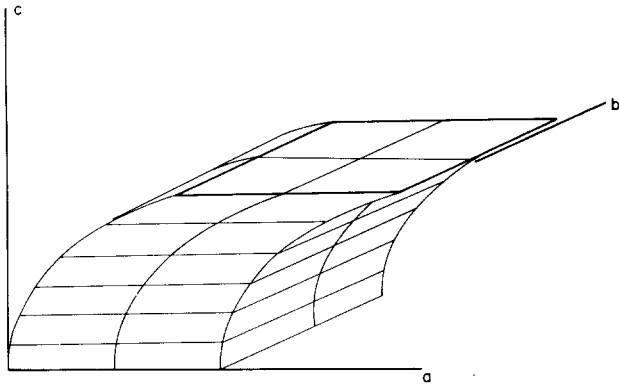


Fig. 27. A zone of heterogeneous simple shear produced by the rank-3 tensor discussed in the text.

recorded at unit depth, so that only a limited range of depths are geologically realistic. This range may be changed by changing the value of the non-zero element.

As a second example, the rank-3 tensor

$$\begin{bmatrix} 0 & 0 & 0 & | & 0 & 0 & 0 & | & 0 & 0 & 1 \\ 0 & 0 & 0 & | & 0 & 0 & 0 & | & 0 & 0 & 0 \\ 0 & 0 & 0 & | & 0 & 0 & 0 & | & 0 & 0 & 0 \end{bmatrix}$$

produces a zone of heterogeneous simple shear (Fig. 27), when substituted for  $\mathbf{U}$  in equation (84). In both of these examples, the output displacement tensor corresponding to each input position vector must be added to identity tensor and a rigid translation must be added in order to achieve the final state. The translational component must be calculated independently, using, for example the compatibility conditions.

## CONCLUSIONS

I have adopted a spatial-geometric approach to the mathematical specification of geological strain patterns. The geometric concepts of the stress and deformation ellipsoids are well established in structural geology. However, an ellipsoidal surface may be associated with every tensor. The spatial-geometric approach is greatly facilitated by the use of graphic facilities attached to digital computers but is also suitable for use on location in the field with the aid of an orthographic orientation net.

The basic orthographic construction in two dimensions is similar to the operation of Tissot's indicatrix in cartography. It also resembles the constructions in Fig. 7.3 of Means (1976) and Hobbs *et al.* (1976), fig. 1.5. It is easily extended to three dimensions and is applicable to rotational deformations.

The method of formulating tensors and the notation used in this paper is logical and internally consistent. Some readers may have misgivings about the use of 1-2-3 for general reference axes and the preservation of  $X$ - $Y$ - $Z$  for the principal axes.  $X$ - $Y$ - $Z$  are often used in continuum mechanics as subscripts denoting arbitrary reference axes in the initial state. However the phrase

" $XY$ -plane of the deformation ellipsoid . . ." is so well established in the geological literature that an attempt to substitute " $12$ -plane . . ." would certainly fail.

Part II of this paper will deal with the practical applications of the above theory to rocks.

*Acknowledgements*—This paper is based on part of my Ph.D. treatise (De Paor 1981). Although essentially unsupervised, I was assisted by many people, particularly W. E. Nevill, J. R. Andrews and J. De Paor, and funded partially by the Irish Department of Education. I presented parts of this paper to many different meetings of the Tectonic Studies Group and am indebted to its members for raw data, laboratory and computing facilities and floor space. The constructive criticisms of the external examiner, D. Sanderson, were appreciated. P. Cobbold and W. D. Means read an earlier draft and made many helpful suggestions which greatly improved the final version. The final draft also benefited from meetings with D. Sanderson, as part of a Joint Study Programme (No. 244) funded by the EEC.

## REFERENCES

- Bates, R. L. & Jackson, J. A. (Eds) 1980. *Glossary of Geology* 2nd Ed., American Geological Institute, Virginia.
- Choi, C. Y. & Hsü, T. C. 1971. Mohr circles for large and small strains in two-dimensional deformations. *J. Strain Anal.* **6**, 62–69.
- De la Hire, P. H. 1685. *Sectiones Conicae in Novem Libros Distributae*, . . . Stephanum Michallet, Parisiis.
- De Paor, D. G. 1979. The use of stereovectors in structural and engineering geology. *Tectonophysics* **60**, T1–T6.
- De Paor, D. G. 1981a. Strain analysis using deformed line distributions. *Tectonophysics* **73**, T9–T14.
- De Paor, D. G. 1981b. Geological strain analysis. Unpublished Ph.D. thesis, National University of Ireland.
- Durelli, A. J., Phillips, E. A. & Tsao, C. H. 1958. *Introduction to the Theoretical and Experimental Analysis of Stress and Strain*. McGraw-Hill, New York.
- Elliott, D. 1970. Determination of finite strain and initial shape from deformed elliptical objects. *Bull. geol. Soc. Am.* **81**, 2221–2236.
- Ericksen, J. L. 1960. Tensor fields. *Handbuch der Physik* **3**, 794–858.
- Flinn, D. 1962. On folding during three dimensional progressive deformation. *Q. Jl geol. Soc. Lond.* **118**, 385–433.
- Flinn, D. 1978. Construction and computation of three-dimensional progressive deformations. *J. geol. Soc. Lond.* **135**, 291–305.
- Flinn, D. 1979. The deformation matrix and the deformation ellipsoid. *J. Struct. Geol.* **1**, 299–307.
- Fung, Y. C. 1977. *A First Course in Continuum Mechanics*. Prentice-Hall, New Jersey.
- Hilton, H. 1917. The use of the orthographic projection in crystallography. *Miner. Mag.* **18**, 122–129.
- Hobbs, B. E. 1971. The analysis of strain in folded layers. *Tectonophysics* **11**, 329–375.
- Hobbs, B. E., Means, W. D. & Williams, P. F. 1976. *An Outline of Structural Geology*. Wiley, New York.
- Lisle, R. J. 1982. A simplified work scheme for using block diagrams with the orthographic net. *J. Geol. Education* **29**, 81–83.
- Lister, G. S. & Williams, P. F. 1983. The partitioning of deformation in flowing rock masses. *Tectonophysics* **92**, 1–34.
- Malvern, L. E. 1969. *Introduction to the Mechanics of a Continuous Medium*. Prentice-Hall, New Jersey.
- Matthews, P. E., Bond, R. A. B. & Van der Berg, J. J. 1974. An algebraic method of strain analysis using elliptical markers. *Tectonophysics* **24**, 31–67.
- McIntyre, D. B. & Weiss, L. E. 1956. Construction of block diagrams to scale in orthographic projection. *Proc. Geol. Ass.* **67**, 142–155.
- Means, W. D. 1976. *Stress and Strain*. Springer, New York.
- Means, W. D. 1982. A new Mohr circle construction for finite strain. *Tectonophysics* **89**, T1–T6.
- Means, W. D. 1983. Application of the Mohr circle construction to problems of inhomogeneous deformation. *J. Struct. Geol.* **5**, 279–286.
- Means, W. D., Hobbs, B. E., Lister, G. S. & Williams, P. F. 1980. Vorticity and non-coaxiality in progressive deformations. *J. Struct. Geol.* **2**, 371–378.
- Nye, J. F. 1951. *Physical Properties of Crystals*. Clarendon Press, Oxford.
- Owens, W. H. 1973. Strain modification of angular density distributions. *Tectonophysics* **16**, 249–261.

- Prager, W. 1961. *Introduction to Mechanics of Continua*. Dover Publ. Inc., N.Y.
- Phillips, F. C. 1954. *The Use of Stereographic Projection in Structural Geology*. Edward Arnold, London.
- Ragan, D. M. 1973. *Structural Geology* (2nd Ed.). Wiley, N.Y.
- Ramberg, H. 1975. Particle paths, displacement and progressive strain applicable to rocks. *Tectonophysics* **28**, 1–37.
- Ramsay, J. G. 1967. *Folding and Fracturing of Rocks*. McGraw-Hill, New York.
- Ramsay, J. G. 1980. Shear zone geometry: a review. *J. Struct. Geol.* **2**, 83–99.
- Ramsay, J. G. & Graham, R. H. 1970. Strain variation in shear belts. *Can. J. Earth Sci.* **7**, 786–813.
- Rankine, W. J. M. 1851. Laws of the elasticity of solid bodies. *Camb. Dubl. Math J.* **6**, Papers 67–101.
- Robin, P.-Y. F. 1977. Angular relationships between host and exsolution lamellae and the use of the Mohr circle. *Am. Miner.* **62**, 127–131.
- Sanderson, D. 1974. Patterns of boudinage and apparent stretching lineation developed in folded rocks. *J. Geol.* **82**, 651–661.
- Skjerna, L. 1980. Rotation and deformation of randomly oriented planar and linear structures in progressive simple shear. *J. Struct. Geol.* **2**, 101–109.
- Thompson, Sir W. & Tait, P. G. 1867. *Treatise on Natural Philosophy Vol. 1*. Oxford, England.
- Tissot, M. A. 1881. *Memoire sur la Representation des Surfaces et Les Projections des Cartes Geographiques*. Paris.
- Treagus, S. H. 1981. A simple-shear construction from Thompson & Tait (1867). *J. Struct. Geol.* **3**, 291–293.
- Treagus, J. E. & Treagus, S. H. 1981. Folds and the strain ellipsoid: a general model. *J. Struct. Geol.* **3**, 1–17.
- Truesdell, G. & Toupin, R. 1960. The classical field theories. *Handbuch der Physik* **3**, 226–793.
- Wahlstrom, E. E. 1951. *Optical Crystallography* (2nd Ed.). Wiley, New York.
- Wright, F. E. 1911. *The Methods of Petrographic-microscopic Research*. The Carnegie Institute, Washington.